The Sensitivity of a General Circulation Model to Large Scale Vegetation Changes

by
Thomas N. Chase

Department of Atmospheric Science
Colorado State University
Fort Collins, Colorado

National Park Service Contract No. 0479-8-8001
National Science Foundation Grant No. ATM-930675
Roger A. Pielke, P.I.

Colorado State University

Department of Atmospheric Science

Paper No. 581

THE SENSITIVITY OF A GENERAL CIRCULATION MODEL TO LARGE SCALE VEGETATION CHANGES

Thomas N. Chase

Department of Atmospheric Science
Colorado State University
Fort Collins, Colorado
Summer 1995

Atmospheric Science Paper No. 581

ABSTRACT

THE SENSITIVITY OF A GENERAL CIRCULATION MODEL TO LARGE SCALE VEGETATION CHANGES

Methods have recently become available for estimating the amount of leaf area at the surface of the earth using satellite data. Also available are modeled estimates of what global leaf area patterns would look like should the vegetation be in equilibrium with current local climatic and soil conditions. The differences between the actual vegetation distribution and the potential vegetation distribution may reflect the impact of human activity on the earth's surface. In order to examine model sensitivity to changes in leaf area index (LAI), global distributions of maximum LAI were used as surface boundary conditions in the NCAR Community Climate Model (CCM2) coupled with the Biosphere Atmosphere Transfer Scheme (BATS). Results from 10-year ensemble averages for the months of January and July indicate that the largest effects of the decreased LAI in the actual LAI simulation occur in the Northern Hemisphere winter at high latitudes despite the fact that direct LAI forcing is negligible in these regions at this time of year. This is possibly a result of LAI forcing in the tropics which has long ranging effects in the winter of both hemispheres. An assessment of the Asian monsoon region for the month of July shows decreased latent heat flux from the surface, increased surface temperature, and decreased precipitation with the actual LAI distribution. While the statistical significance of the results has not been unambiguously established in these simulations, we suspect that an effect on modeled general circulation dynamics has occurred due to changes

of maximum LAI suggesting that further attention needs to be paid to the accurate designation of vegetation parameters. The incorporation of concomitant changes in albedo, vegetation fractional coverage, and roughness length is suggested for further research.

Thomas N. Chase
Department of Atmospheric Science
Colorado State University
Fort Collins, Colorado 80523
Summer 1995

DEDICATION

Dedicated to a Brother

Robert A. Chase

1963-1995

ACKNOWLEDGEMENTS

I thank Dr. Roger Pielke for starting me off on this project and for providing a jumpstart when necessary. I would also like to thank Dr. Timothy Kittel for his considerable input in many areas over the past few years. Thank to Drs. Baron and Randall for serving on my thesis committee.

To Dr. Copeland, Dr. Lee, Dr. Zeng, and soon to be Drs. Finley and Eastman - thanks for all the help along the way. Thanks to Dr. Jennifer Cram for getting me off to a good start and to Dallas McDonald for sorting out the mess at the end. I thank the CCM group for answering my questions and Dr. Rama Nemani and Dr. Steve Running for providing the LAI data used here. For everything else I thank my parents.

Support for this research was provided by the National Park Service through Contract No. 0479-8-8001 and the National Science Foundation under Grant No. ATM-930675. I would like to thank NCAR for providing computer time and access to CCM2. NCAR is partially supported by the National Science Foundation.

TABLE OF CONTENTS

LIST OF TABLES

LIST OF FIGURES

Chapter 1

INTRODUCTION

It is generally agreed that the extent and type of vegetation covering the earth has changed dramatically due both to natural and anthropogenic causes. Estimation of natural vegetation change has been attempted in several ways. Street-Perrott et al. (1990) have shown data to support the conclusion that 8000 years ago, monsoon westerlies penetrated farther north into Asia allowing an increase of biomass in more northerly latitudes than are seen today. Geological evidence supports the assertion that plant life was abundant in many parts of the Sahara as a result of the increased moisture supplied by these monsoon circulations. Overpeck (1993), based on paleo-data for the past 18,000 years has calculated that natural changes of near surface air temperature on the order of a few degrees centigrade has forced large changes in vegetation cover. This natural variability in vegetation cover and its relation to natural variations in climate makes estimating human impacts even more challenging.

Estimates of human impact on the surface characteristics of the earth are extensive despite their problematic nature. Matthews (1983) discusses the subjective nature of previous landuse compilations including the difficulty of comparing different classification schemes. Classification usefulness also varies with purpose. Gornitz (1987) gives an account of the effort to estimate the amount of land area which has been turned from forest to cultivated land. These estimates range from 725 $\times 10^3$ to km^2 931 $\times 10^3$ km^2. She also estimates current rates of deforestation as a function of population growth. Houghton (1994) reviews other methods of estimating current

land-use changes including the number of fires burning in the tropics or the number of regular land patches surrounded by forested areas. Williams (1990), in a review of various techniques for estimating deforestation, points out that adequate records were seldom kept and so historical land cover estimates are probably very rough and inadequate. These papers all illustrate that the methods used are crude and results uncertain. Perhaps all that can be hoped for is a qualitatively reasonable map of land use changes rather than a definitive one.

While it is obvious that human intervention and changes in past climates have had impacts on vegetation, there is also observational evidence that vegetation can have an impact on climate (Pielou, 1991). Meher-Homji (1991), in a review of the impacts of deforestation on local precipitation found that surface temperature fluctuates more in non-forested regions as opposed to forested areas. He also finds evidence that with decreasing forest comes decreasing precipitation. The impact of vegetation on the atmosphere is inherently difficult to observe because of the timescales involved and the lack of adequate analogs for comparison. This leaves the topic in a state of contention and encourages experiments with numerical models.

Vegetation affects the atmosphere in very complex, non-linear ways and attempts have been made to understand these interactions and to describe them numerically. First, vegetation cover has an impact on the reflectance of the earth's surface. In general, vegetation is darker than bare soil and so absorbs more short wave radiation at the surface subsequently affecting the energy balance at the earth's surface. A plant canopy also shades the earth's surface and, in a dense canopy, the leaves interior to the canopy.

Vegetation affects the roughness of the surface as well. Higher, denser vegetation can enhance the transfer of turbulent fluxes of heat and momentum from the surface of the earth to the atmosphere. Denser vegetation allows for more surface area to interact with the atmosphere.

The impact of vegetation can also be expected to be seen in the surface water balance. Vegetation can intercept more water and evaporate it directly back to the atmosphere. More water may be stored in plants and soils stabilized by root structures and so surface runoff can be reduced. Vegetation facilitates the tapping of water reserves from below the surface via rooting systems and so allows extra moisture into the atmosphere via transpiration. This will affect the partitioning of surface heat fluxes which in turn has an impact on the development of the planetary boundary layer and the atmosphere at large. Vegetation can also have an indirect impact on planetary albedo by altering soil moisture content. Generally, moister soils are less reflective than dry soils (Otterman, 1977). The numerical model must account for all the above factors in descriptions of the surface.

1.1 Modeling Studies

Climate modelers have become increasingly aware of the importance of the specification of the lower boundary to model simulations in recent years. Reviews of these experiments (e.g., Mintz, 1984; Garratt, 1992; Rowntree, 1988) show that the surface designation in a numerical model can have quite large and significant impacts on modeled climate.

In numerical models the complicated physical mechanisms of vegetation and its interaction with the atmosphere must be simplified to a few parameters. The first experiments designed to test the impact of vegetation change on climate used very simple methods to handle vegetation changes. For example, many experiments have estimated the impacts of vegetation change simply as a change in surface albedo (e.g., Charney, 1975; Sagan et al. 1979; Potter et al. 1981; Henderson-Sellers and Gornitz, 1984) implicitly assuming that the largest impact due to vegetation would be its effect on reflectivity. All the above experiments found that the designation of surface albedo had a significant effect on numerical climate, though to differing degrees, and were highly dependent on the magnitude of roughly estimated albedo

changes. An increased albedo generally decreased surface temperatures and decreased and altered precipitation distribution. In a more recent study, Meehl (1994) has found a relationship between specification of surface albedo and the strength of the summer monsoon based on the review of several GCM experiments. Simulated monsoons were strengthened when albedo changes caused larger contrasts between land and sea surface temperatures.

Similar experiments have been performed in an effort to ascertain the effect of a change in roughness length due to deforestation with both regional and global changes taken into account. Surface roughness was found to have an impact on water vapor convergence and precipitation distribution in the model (e.g., Sud and Smith, 1985; Sud et al., 1988).

The regional impacts of limited area vegetation changes have also been addressed in model experiments. Much effort has been put into the regional and global effects of Amazonian deforestation. Garratt (1992), in a review of these experiments shows that the common elements among those experiments with a land surface scheme includes a reduced hydrological cycle and an increased near-surface air temperature in the region of the change. Globally there are few averaged effects and it has been noted that realistic vegetation changes may not be able to force climate on a global scale but might be capable of altering regional scale climate (Henderson-Sellers, 1984).

The difficulty with the above cited experiments is the relative simplicity of the description of vegetation and the lack of interaction or feedback among the various processes being explored. Albedo and roughness length distributions are held constant. Soil moisture does not interact with the dynamical changes induced in a model. It has been shown (Jacobs and DeBruin, 1992) that because of the nonlinearity of the problem, feedbacks from atmosphere can have a large effect on the final model solution. In this case it was shown that for a 'deforestation' experiment,

estimates of transpiration could be in error by a factor of 2 or 3 if feedbacks from the planetary boundary layer are ignored. Clearly more sophisticated accounts of the interaction between the surface and atmosphere are necessary if we are to have confidence in the the modeled effects of vegetation perturbations.

More complicated land surface models are now available. They describe the land surface and vegetation changes using more interactive parameters recognizing that the role of vegetation is not limited to the effect on surface albedo or on the relative roughness of the surface. Attempts to allow vegetation to interact with the atmosphere, to model the effects of transpiration modulation by the canopy and effects on the surface water balance mean that a measure of the amount of active biomass in a region must be accounted for. This has led to the inclusion of a widely used variable, Leaf Area Index (LAI) in the description of the planetary surface. Defined as the ratio of leaf area to surface area in a vertical column, LAI is a representation of the density of vegetation at the surface. The primary role of LAI is in regulating the amount of transpiration from the surface and thereby controlling the partition of surface heat fluxes. The larger the leaf area in the column, the more evapotranspiration that can occur. Also, LAI regulates light extinction in the canopy so that generally a larger value indicates less light reaching the soil surface. Since stomatal conductance is also a function of light (Denmead and Miller, 1976), LAI directly affects the stomatal conductance of individual leaves as well as the integrated conductance of the canopy.

Studies have been performed in an attempt to unravel the properties of vegetation and combinations of properties which are most important in a given situation. For example, in a recent study of statistical-dynamical models of the earth's surface, Collins and Avissar (1994) using Fourier Amplitude Sensitivity testing found that the distribution of surface heat fluxes could be explained mostly by variations in stomatal conductance and roughness length. Stomatal conductance was found to

have the greatest significance in its effect on both latent and sensible heat fluxes. The surface roughness was of secondary significance and mostly important for situations with low environmental wind speeds. Interestingly, surface albedo was found to be insignificant in the explanation of both latent and sensible heat flux variance though vegetation albedo had a larger effect. LAI was found to be significant to the sensible heat flux only under circumstances where the surface is partially vegetated. Henderson-Sellers (1993) using a stand alone ecosystem model found the model to be highly sensitive to roughness length and relatively insensitive to LAI designation.

However, Li and Avissar (1993), found that LAI was the most important variable contributing to errors due to neglecting sub-grid scale land surface variability. Zhang (1994) found that a dense vegetation cover effectively made surface heat fluxes independent of ground surface conditions, particularly soil moisture. This was based on a vegetation fraction designation but presumably high values of LAI should have a similar effect. Bonan et al. (1993), using a fairly complex land surface parameterization found that subgrid heterogeneity in the LAI field was the primary cause of surface flux calculation errors for both wet and dry soils. A strong non-linear relationship between LAI designation and these fluxes was also apparent. Also noted in this experiment were that many of the effects of increasing leaf area asymptote relatively quickly. For example, most of the influence of increasing leaf area on light extinction occurs at relatively small values of LAI limiting stomatal conductance. However, the area available for energy exchange and water interception increase linearly with leaf area. Clearly, the role of vegetation density and its proxy, LAI, is complex and somewhat ambiguous in parameterizations of surface processes.

Large scale vegetation changes, modeled comprehensively, have been shown to have large impacts on modeled climate. In an experiment of global scale, Bonan et al. (1992), using a relatively complex surface parameterization and an interactive

ocean, found that completely removing the high latitude boreal forests had large effects on the simulated climate. These simulations included changes in other parameters besides LAI such as vegetation fraction, and so included direct radiative forcing due to changes in surface albedo. McGuffie et al. (1995) studied tropical deforestation with a version of the Community Climate Model coupled with BATSIE and a slab ocean model. Because tropical forests were changed to scrub grasslands in this experiment, albedo and roughness length changes were included in the description of deforestation. Results from this experiment showed locally decreased precipitation as a result of tropical deforestation as well as remote effects in mid and high latitudes. Finally, in a study which advances the complexity of the description of surface characteristics to include vegetation structure which interacts dynamically with climate, Henderson-Sellers and McGuffie (1995) find evidence that changes in vegetation due to altered climate feed back into that climate and so must be accounted for.

1.2 Experiment Description

The experiment described below is fundamentally a continuation of past deforestation and land use change numerical experiments. In this case we used the NCAR Community Climate Model (CCM2) general circulation model coupled with the Biosphere Atmosphere Transfer Scheme (BATS) land surface parameterization. We described a change in vegetation globally solely in terms of annual maximum Leaf Area Index (LAI) in order to ascertain model sensitivity to this parameter. The control simulation used a distribution of observed maximum LAI derived from remotely sensed data as a bottom boundary condition. A second run used a distribution of LAI representing the potential maximum LAI sustainable at a site. The derivation of these LAI distributions will be discussed in more detail in Chapter 4.

The two cases were run for a total of 12 years with the results from years 3-12 used for 10-year January and July ensemble averages. The first two years

were ignored as spin-up time. Though the total soil moisture field had not quite equilibrated by the third year, the differences were small and it was felt to be more important to have two 10-year samples to compare. We present results from 10-year averaged Januarys and Julys as well as regional results from southern Asia in July.

Chapter 2

DESCRIPTION OF CCM2

2.1 General Model Description

The NCAR CCM2 is a primitive equation general circulation model in which variables are expressed in terms of series of spherical harmonics and the governing equations are solved in spectral space in the horizontal. Finite differences are used in the vertical. The spectral truncation in this case is triangular allowing 42 zonal wavenumbers (T42). This corresponds to a grid increment of approximately 2.8 degrees longitude by 2.8 degrees latitude (128 by 64 points in the horizontal). There are 18 vertical levels in a hybrid sigma coordinate system where sigma levels are used near the surface and blend into a pressure coordinate system at some point above the surface. The model has a rigid lid at around 3mb. The model uses climatological sea-surface temperatures and topography averaged from a 1 degree by 1 degree data set.

CCM2 includes a diurnal as well as an annual radiation cycle (Briegleb, 1992). The shortwave radiation parameterization uses a delta Eddington approximation to compute solar heating rate every model hour. The parameterization includes 18 spectral intervals, gas absorption (H_2O, CO_2, O_2, O_3), and clouds which interact with radiation fluxes depending on cloud droplet properties which are specified as functions of altitude and latitude. Multiple reflections from surface and clouds are accounted for, as are overlapping clouds. Clouds can form in all tropospheric levels above the first and cloud fraction is calculated as a function of relative humidity, vertical motion, static stability, and convective precipitation rate.

The parameterization of the planetary boundary layer (PBL) in CCM2 accounts for dry convection by adjusting for non-local transport in the boundary layer (Holtslag and Boville, 1993). The parameterization calculates the PBL height, diffusion profiles and turbulent transport.

A mass flux moist convective scheme is included in CCM2 (Hack, 1994). The parameterization adjusts moist static energy over three adjacent vertical layers starting from the surface and continuing throughout the troposphere. The convection scheme uses perturbation quantities from the PBL parameterization to diagnose stability and as such the two schemes are coupled. The large scale horizontal transport of water uses a semi-lagrangian (not spectral) method. A detailed general overview of CCM2 can be found in Hack et al. (1993).

2.2 The Biosphere Atmosphere Transfer Scheme (BATS)

The Biosphere Atmosphere Transfer scheme as coupled to the NCAR CCM2 (BATS1E) has been used in these experiments. BATS is a simple land surface parameterization which includes a single vegetation canopy layer and three soil layers. The BATS parameterization computes heat flux partitioning from vegetation and bare soil surfaces, and water budget values and feeds them into the atmospheric portion of the model.

In BATS, the earth is divided among 18 surface types and representative values of 18 parameters describing properties of vegetation such as maximum and minimum stomatal resistance, maximum and minimum leaf area index, and soil properties are assigned. BATS divides each grid cell into a vegetated and non-vegetated fraction. Vegetation fraction varies regularly with season as a function of sub-surface soil temperature. There is no provision for the effect of soil water (or lack thereof) on vegetation cover. The fluxes of heat and moisture are proportional to the gradient of temperature and vapor pressure between the surface and the first atmospheric level. Vegetation fraction is reduced in the presence of snow.

The Leaf Area Index (LAI) calculation is simple and seasonally varying. LAI is a measure of the ratio of leaf area in a model grid cell to surface area in the cell. For each vegetation type a maximum and a minimum value of single sided LAI is assigned. The actual value of LAI used in the model is computed similarly to the vegetation fraction with the value of LAI varying between the maximum and minimum allowed LAI assigned to the grid box as a function of the sub-surface soil temperature according to the equation.

$$\text{LAI} = \text{MAXLAI} + (\text{MINLAI} - \text{MAXLAI}) * (1.0 - \text{SEASONAL PARAMETER}) \tag{2.1}$$

where

$$\text{SEASONAL PARAMETER} = 1 - 0.0016 * (298.0 - Tg_2)^2 \tag{2.2}$$

for Tg_2 between 273.16° and 298.0° and where Tg_2 is the second ground layer temperature. Again, no provision is made for the effect of soil water availability on the distribution of LAI.

In nature, LAI is related to other vegetation characteristics. For example, larger values of LAI correspond generally with decreased albedo and higher values of roughness length. In the BATS parameterization, altering the values of maximum LAI by itself does not affect either the surface albedo or roughness length of the vegetation because each of these is specified independently. However, stomatal resistance is directly affected by specification of LAI through the extinction function of light through the canopy leading to greater extinction values (e.g., Li and Avissar, 1994),and an increased resistance to transpiration. Canopy air temperature and vegetation temperature are also functions of LAI in the BATS parameterization.

2.3 Actual Vs. Potential Vegetation and its Representation

A control simulation was performed using a maximum LAI distribution developed by Nemani et al. (1995) based on Normalized Difference Vegetation Index (NDVI) data retrieved from satellite observations. NDVI is the difference between infrared and visible reflectances normalized by their sum. This index has been used to estimate the amount of photosynthetically active material in the canopy (e.g., Sellers et al., 1985; Goward et al., 1986). It has been found (e.g., Nemani and Running, 1989) that a relationship exists between NDVI data and leaf area of the canopy. Nemani et al. (1995) used seven years of NDVI data to reduce the effects of cloud contamination and annual variability. Separate relationships between NDVI and LAI were used for grasses, needleleaf trees, and broadleaf trees. This is an estimate of the maximum vegetation density as it actually appears today (Fig. 1a). The experiment with this LAI distribution is titled actual LAI or actLAI.

In a second simulation, a distribution of maximum LAI entitled potential LAI or potLAI was used as a comparison case. Nemani and Running (1989) presented a technique of using a simple ecosystem model to arrive at equilibrium values of leaf area based on inputs from a climatological atmosphere and soil type. Maximum sustainable transpiration at a site is calculated through an iterative technique where transpiration, soil water holding capacity and precipitation must come into balance. When this balance is achieved, maximum transpiration is reached. Because total leaf area regulates transpiration, maximum LAI is directly related to this total transpiration. They ran the ecosystem model using climatological information on a 0.5° latitude/longitude grid to obtain an estimated global distribution of maximum sustainable LAI which represents the potential leaf density a site could support assuming equilibrium with current climate (Fig. 1b). This estimate of potential LAI does not account for effects of nutrient limitation and natural disturbances (such as forest fires) on vegetation density. While these assumptions can lead to LAI

errors in for some environments, this method provides a good first order estimate of potential LAI distribution under current climate. Nemani et al. (1995) discuss the derivation of these maximum LAI distributions in more detail.

The difference between actual and potential LAI distributions can be taken as a direct estimate of one aspect of human impact on vegetation. It should be noted that the observation of surface characteristics from satellites is imprecise (e.g., Gamon et al., 1995). Imperfect knowledge of soil type, soil moisture, and vegetation type globally can introduce errors into LAI data sets. Modeled distributions of potential LAI such as used in this study are subject to the assumptions inherent in the model used and datasets obtained by varying methods can yield contradictory results (see, for example, the discussion in Neilson, 1993). Some differences between these datasets could be due to differences in method used in deriving them. One is satellite observed (actual LAI), the other is calculated (potential LAI) through a water balance model. We look at our experiment as a plausible perturbation in global leaf area in magnitude and distribution designed to test the sensitivity of the model to this parameter.

These maximum LAI distributions were averaged to the CCM2 grid using a 5 nearest neighbor aggregation (a 2.5° square area; Figure 2.1). Because model values of LAI vary with ground temperature between minimum and maximum values, LAI values were generally not at their maximum values throughout the simulation. Differences between the two distributions varied seasonally and tended toward zero in the winter hemisphere. Maps of the differences between the two distributions averaged over the ten years for January and July are shown in Figure 2.2. Global land averages in January showed an average LAI of 1.5 for the potLAI case decreasing about 7% to 1.4 in the actLAI case. In July, averaged LAI decreased 16% from 1.9 to 1.6 between the two cases.

While these are fairly small LAI differences when averaged globally, actual differences were concentrated in certain areas. In January, LAI differences were

concentrated below 20° North with the largest differences in Malaysia, southern Asia, southeast Africa, and northern South America (Figure 2.2a). In July, differences are noticeable in the eastern United States, western Europe, Japan, Malaysia, southwest Africa, and northern South America (Figure 2.2b). Most of these were strongly negative (actLAI - potLAI) indicating a decrease in leaf density in these regions from the potential to actual distributions.

It is expected that the maximum direct forcing due to a change in LAI will be in the summer hemisphere and, in an annually-averaged sense, the tropics. In the tropics, LAI differences between the two simulations remained relatively high and constant throughout the year because of a lack of soil moisture dependency in the LAI calculations. Much of the atmospheric heating in the tropics is associated with land masses in Africa, South America, and Indonesia (e.g., Ramage 1968) and is where direct vegetation forcing would be expected to have the largest influence. The magnitude and distribution of heating in this region is a powerful mechanism in generating tropical circulations both in a symmetric sense and for the generation of synoptic-scale waves (e.g., Gill, 1980; Webster, 1983; Meehl, 1993; Hoskins and Karoly, 1981). Both averaged heating and changes longitudinally in the distribution of tropical heating are associated with large changes in the extra-tropical latitudes. Rasmussen and Mo (1993) emphasize the regional character of anomalies due to the 1986-1989 ENSO event and show that the strongest differences in this event were not in alterations in the zonally-averaged circulations but in longitudinal deviations from the average which again affected regions well displaced from the tropics. As previously mentioned, McGuffie et al. (1995) found evidence of mid and high latitude effects due to tropical deforestation. It may be possible that LAI distribution changes alone have a similar effect.

Because LAI is the only forcing variable in the experiment described in this paper, the partitioning between latent and sensible heat fluxes from the surface due

to LAI changes is the primary issue. The question arises as to whether the change in LAI distribution is capable of forcing large enough differences in latent versus sensible heating to fundamentally affect circulations in the summer hemisphere directly, the winter hemisphere indirectly, and the tropics either in magnitude and distribution.

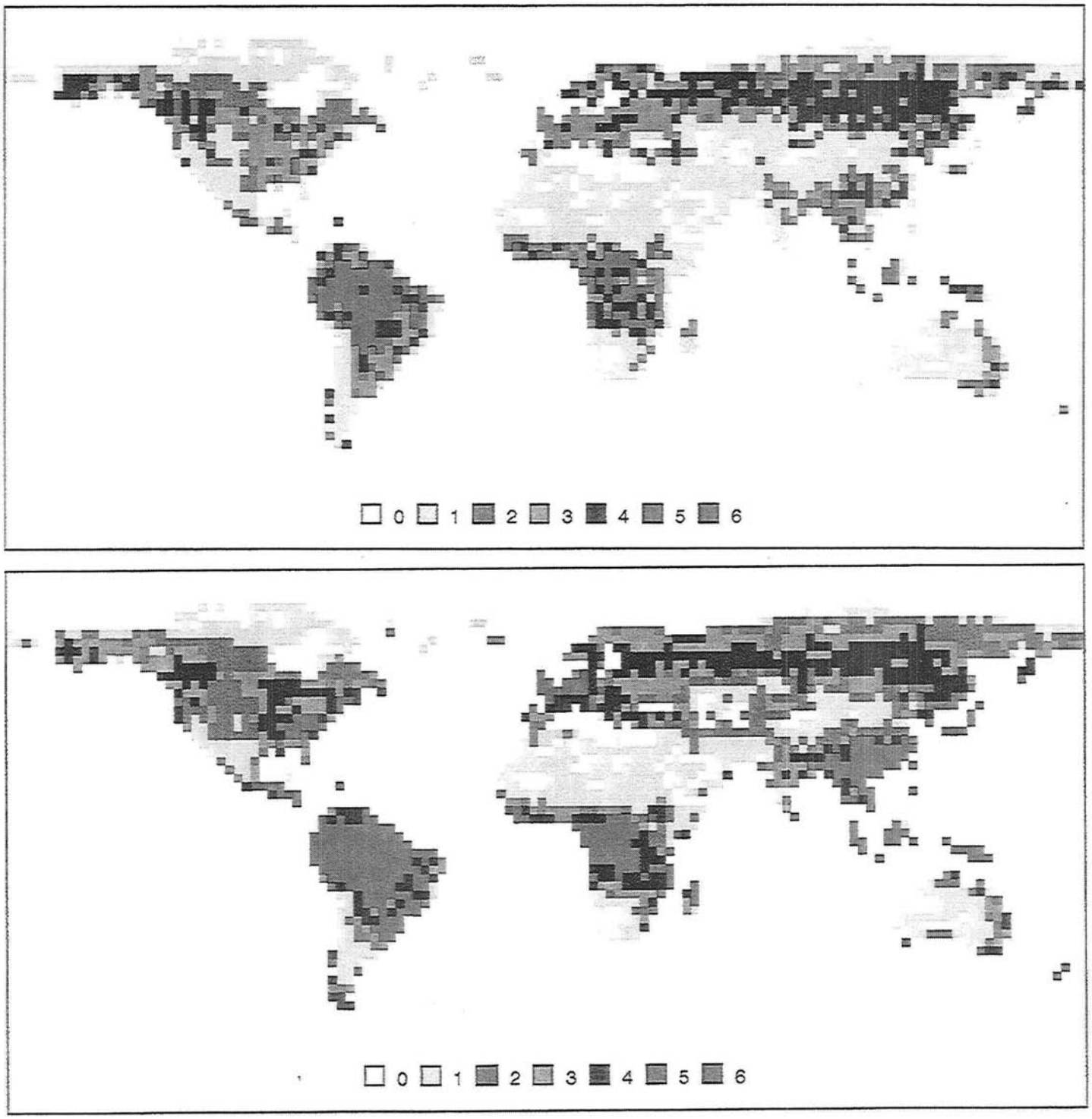

Figure 2.1: Maps of single-sided Leaf Area Index (LAI), (a) actual LAI and (b) potential LAI. LAI values run from 0-6.

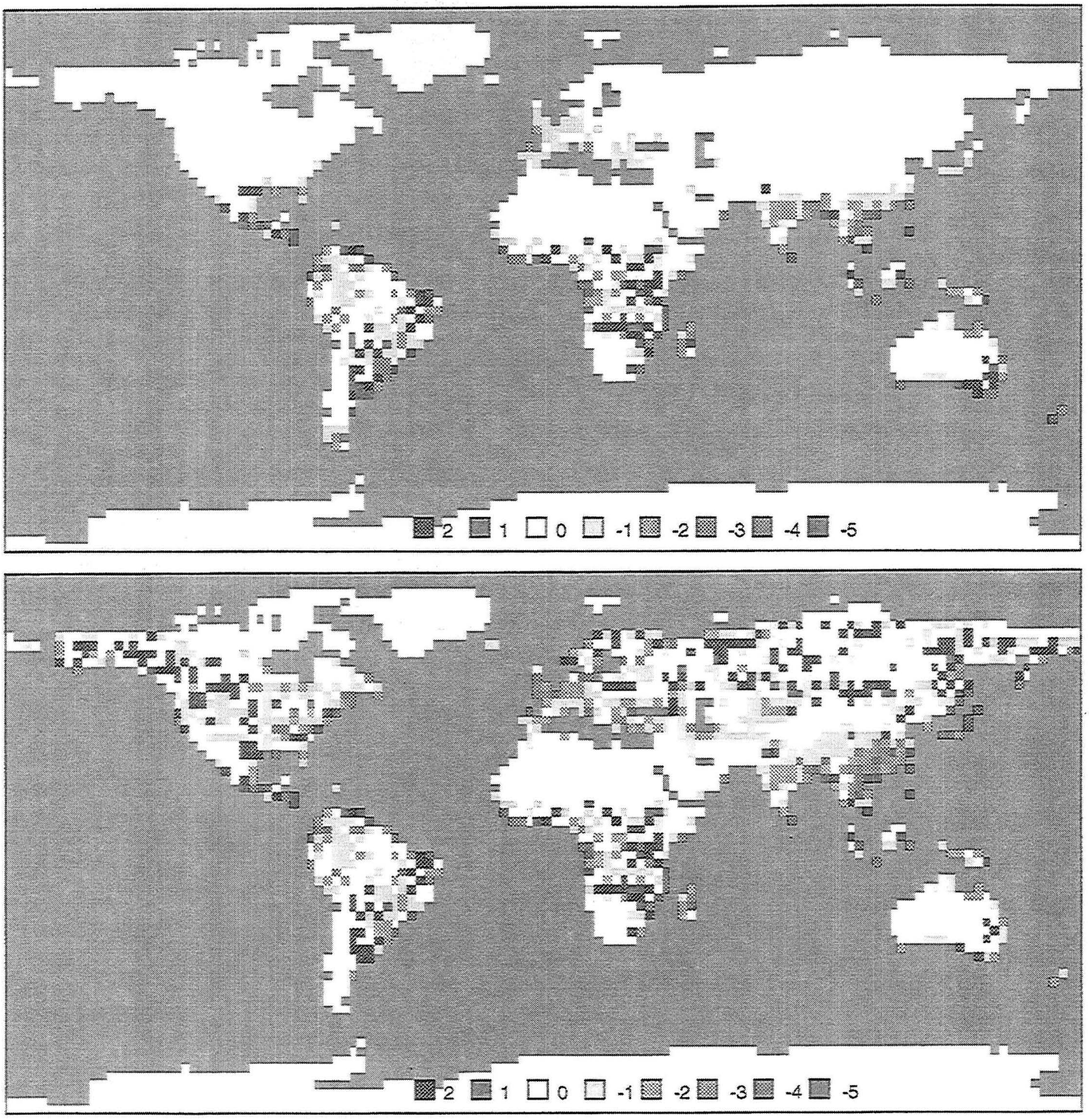

Figure 2.2: Global mean distributions of LAI differences (actLAI - potLAI) for a) January, and b) July.

Chapter 3

RESULTS

3.1 Global Averages

Table 3.1 summarizes differences between globally averaged quantities in the two experiments. Generally, these globally averaged differences are quite small. Average differences over global land surfaces (Table 3.2) are also relatively small though there is a warming over land surfaces of 0.2 K in July in the actLAI case when global differences in leaf area are largest. This is likely a reflection of the decreased evaporation from the surface in the actLAI case of 0.76 (W/m^2) in July.

VARIABLE	*JANUARY*	*JULY*
Maximum 1.5 m Temperature (K)	+0.08	+0.05
Average 1.5 m Temperature (K)	+0.05	+0.05
Sensible Heat Flux (W/m^2)	–0.01	+0.03
Latent Heat Flux (W/m^2)	–0.21	–0.46
Total Clouds (frac)	+0.003	–0.001
Total Precipitation (mm/day)	0.0	-0.02
Incident Solar at Surface (W/m^2)	–0.01	+0.5

Table 3.1: January and July global averages: Summary of differences (actLAI - potLAI).

3.2 Regional Scale

The largest meteorological differences between actual and potential LAI cases in January averages were in the high Northern Hemisphere despite the fact that LAI

VARIABLE	*JANUARY*	*JULY*
Leaf Area Index	–0.17	–0.28
Maximum 1.5 m Temperature (K)	+0.01	+0.17
Average 1.5 m Temperature (K)	-0.03	+0.2
Skin Temperature (K)	+0.05	+0.18
Sensible Heat Flux (W/m^2)	+0.45	–0.01
Latent Heat Flux (W/m^2)	–0.52	–0.76
Short Wave at Surface (W/m^2)	+0.17	–0.01
Total Clouds (frac)	+0.003	+0.001
Total Precipitation (mm/day)	–0.03	+0.02
Runoff (mm/day)	+0.01	0.0
Total Soil Moisture (mm)	–0.12	+0.08

Table 3.2: January and July global land averages: Summary of differences (actLAI - potLAI).

differences were non-existent in these regions at this time of year. Skin temperatures and air temperatures up to the mid-troposphere show large differences above 20° North. The January 1.5 m air temperatures (Figure 3.1) increased over all of the continental United States in the actLAI case relative to the potLAI case, with a maximum warming of more than 5 K. A cooling of similar magnitude occurred in most of eastern Canada. A warming of more than 6 K occurred in the high northern latitudes of Europe and Asia, accompanied by a cooling of several degrees below approximately 55°N. The Southern Hemisphere was relatively unaffected in the near-surface temperature field in January, however smaller magnitude temperature differences between the cases are evident in high southern latitudes in July. Near-surface air temperature differences followed continental outlines presumably because of the constant sea surface temperatures used as boundary conditions in these simulations.

The pattern of January 500 mb height differences filtered to include wavenumbers 1-6 only (Figure 3.2) reproduced the January temperature difference field, indicating that surface temperature differences were due to altered longwave activity

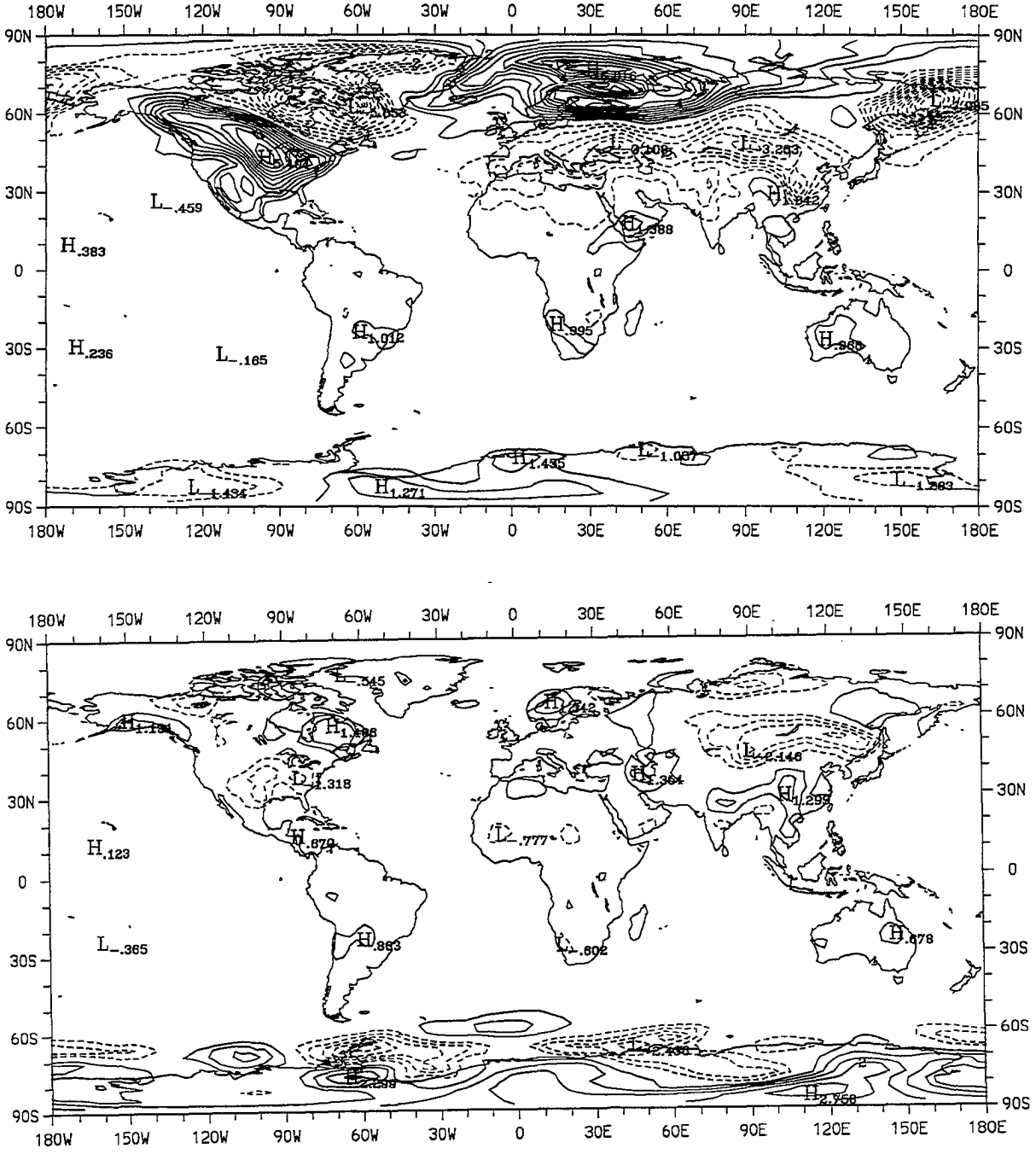

Figure 3.1: Differences in 1.5 m air temperature (actLAI-potLAI) in K for a) January, and b) July. Contours by 0.5.

between the two cases. The similarity in pattern of 500 mb height differences and 1.5 m temperature differences also reflects that temperature differences between the two simulations were present vertically through much of the troposphere.

Total precipitation (Figure 3.3) generally decreases regionally over tropical land surfaces in the actLAI case in January. This decreased precipitation occurs in northern and eastern South America, southern Africa and northeast Australia. Increased precipitation in the actLAI case is seen in central South America, and regions north of Australia. In July, the actLAI case shows decrease precipitation in Southeast Asia and eastern China but a large increase over India. A large increase in precipitation is also seen in Central America in this case. The patterns of precipitation in these regions are quite similar in both the actLAI and potLAI cases indicating that, in large part, the differences in this field are due to increases and decreases in magnitude rather than due to shifts in maxima. Areas of increased precipitation generally are balanced out by areas of decreased precipitation so that there are only small differences between cases in the global average.

3.3 Zonal Averages

In January, the area of peak zonally-averaged precipitation (Figure 3.4) shifted northward slightly in the actLAI case relative to the potLAI case. The maximum value in the precipitation peak was also smaller in the actLAI case by nearly 1.0 mm/day. There was a small decrease in precipitation along the Northern Hemisphere storm tracks in the actLAI case while precipitation increased in most of the Northern Hemisphere subtropics. In July, there were few differences between the two cases for zonally-averaged total precipitation.

Zonal winds are shown in Figure 3.5. There was a small decrease in the magnitude of the Northern Hemisphere 200 mb jet core in January of nearly 2%, while the Southern Hemisphere jet increased slightly in magnitude in the actLAI case. The Northern Hemisphere jet in January also broadened in the actLAI case on the

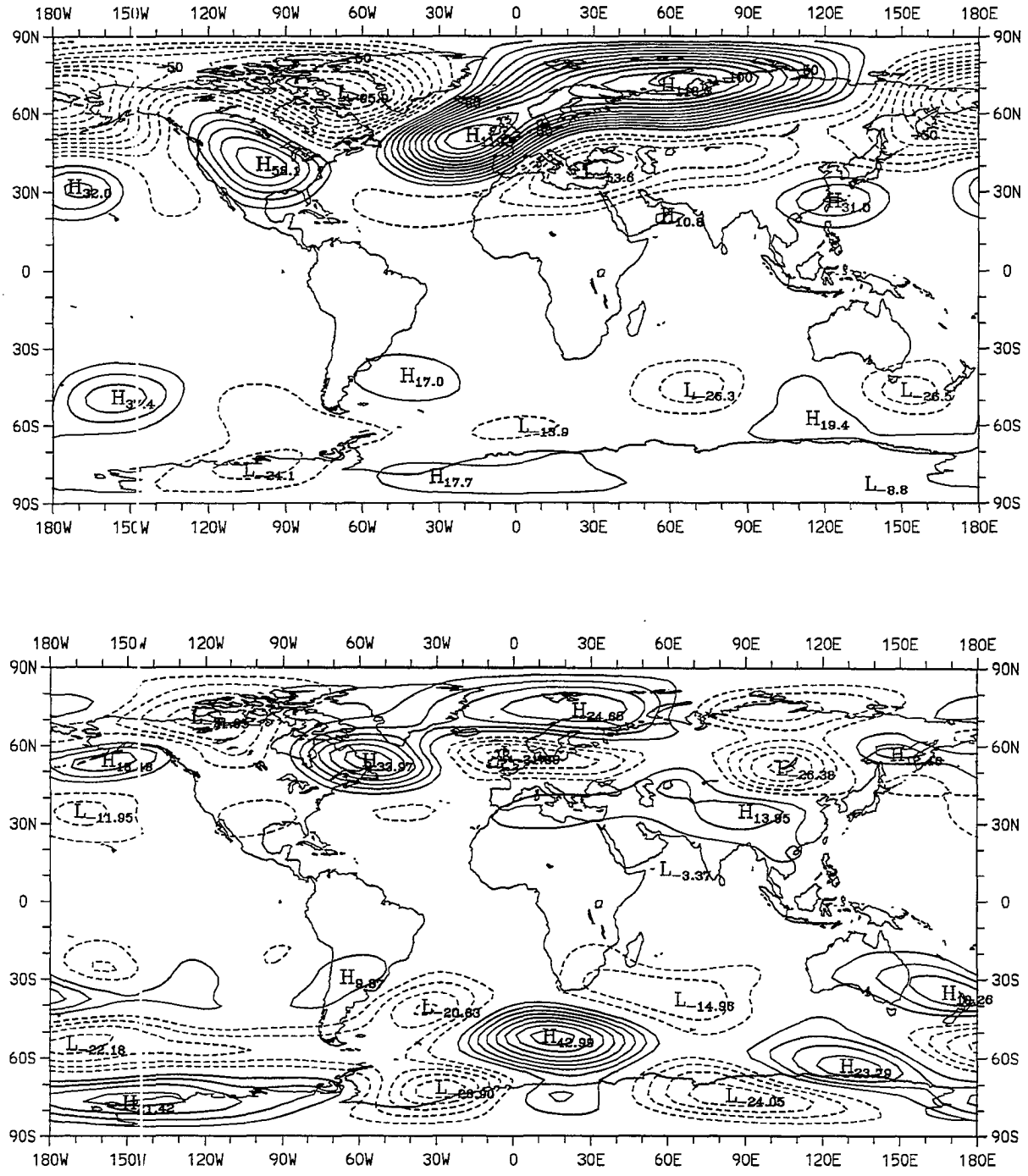

Figure 3.2: Differences in 500 mb heights zonal wavenumbers 1-6 only. (act-LAI-potLAI). a) January contour 10 Pa, and b) July contour 5 Pa.

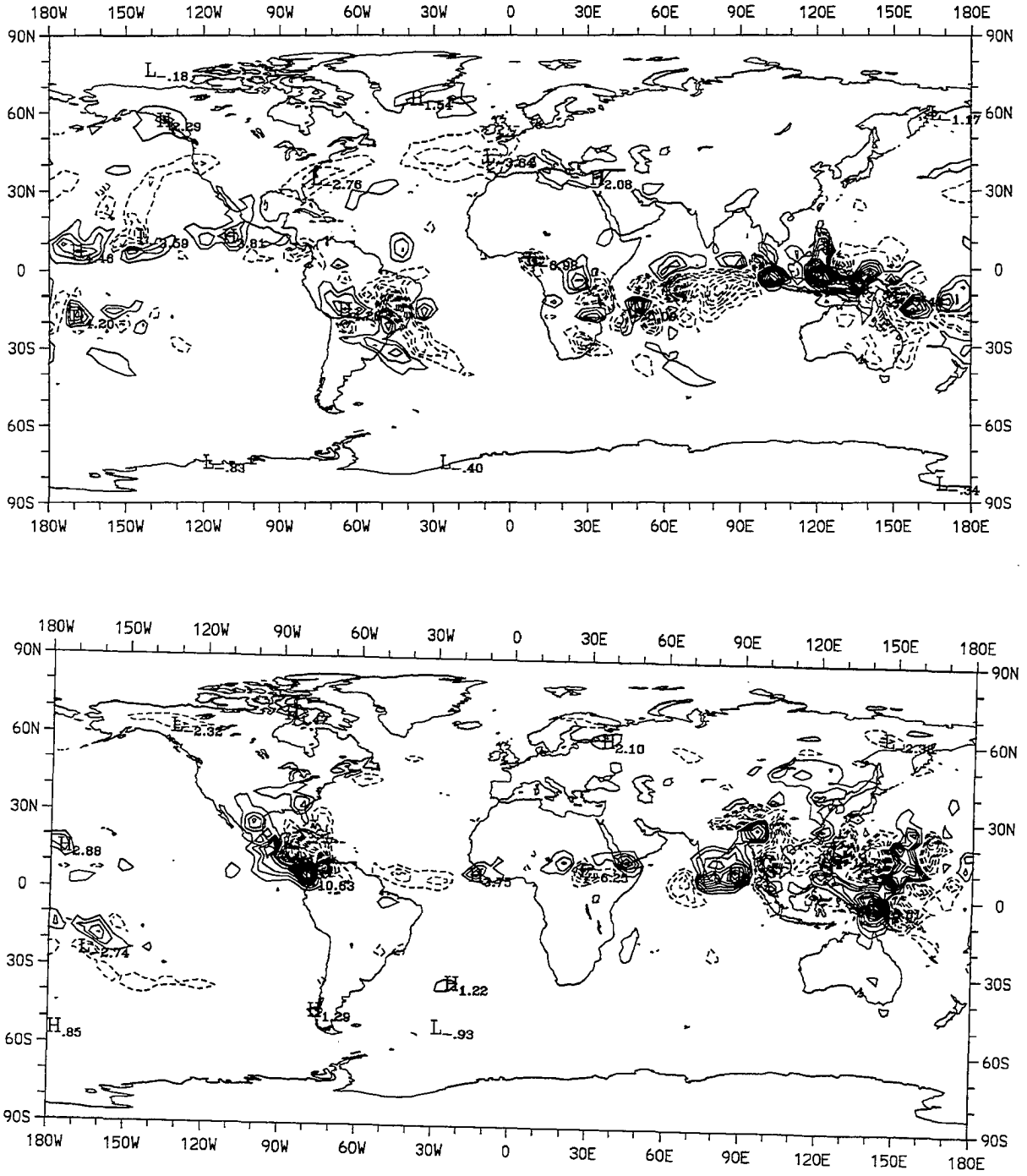

Figure 3.3: Total precipitation differences (actLAI-potLAI). Contour by 1 mm/day for a) January, and b) July.

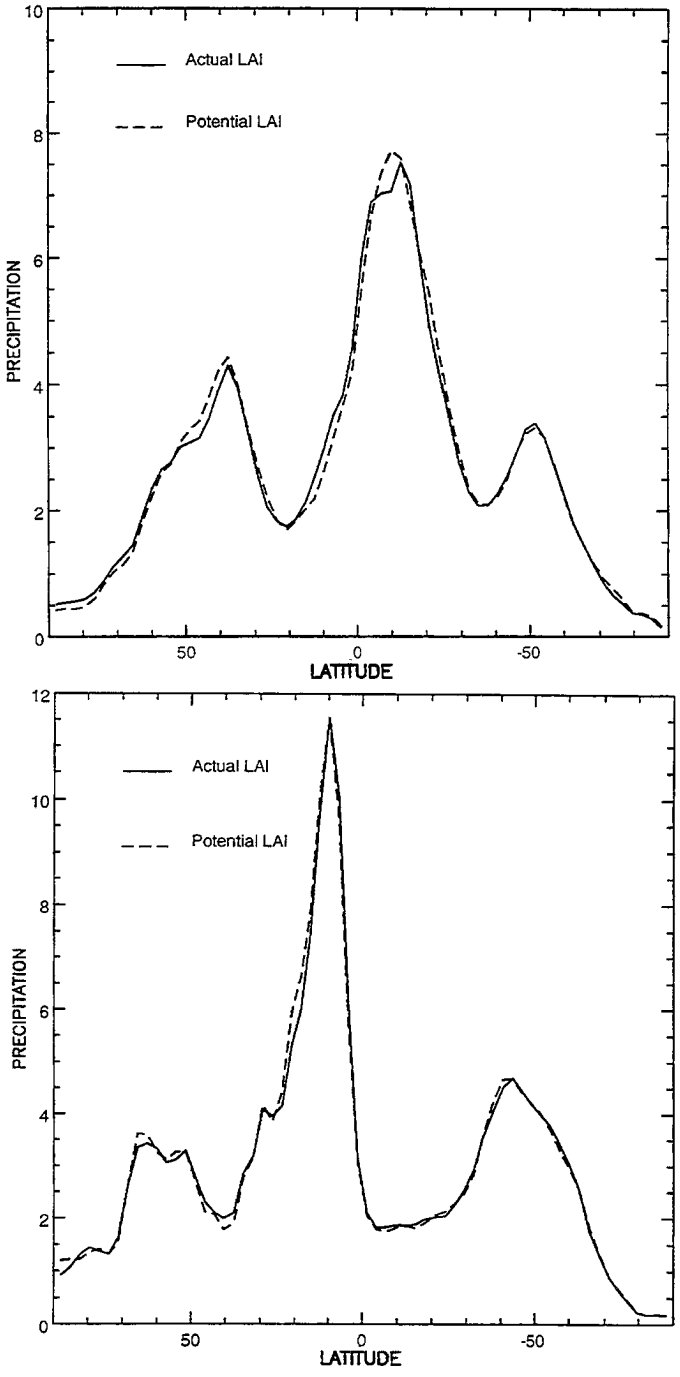

Figure 3.4: Total precipitation vs. latitude in mm/day for a) January, and b) July.

northern side of the jet core. For example, the 20 m/s contour at 200 mb is approximately 1 degree latitude farther north in the actLAI case as compared to the potLAI case while the 25 m/s contour is approximately 3 degrees farther north. Horizontal shear associated with the jet thus decreased in the actLAI case.

The July 200 mb jet had a smaller magnitude in both hemispheres in the actLAI case though the changes were small. Velocity contours around the Northern Hemisphere 200 mb jet remain approximately 2 degrees farther south in the actLAI case indicating that the jet contracted from the pole. This is the opposite of the effect seen in January in the Northern Hemisphere.

Zonally-averaged meridional winds (Figure 3.6) showed a slightly decreased magnitude (6%) in the actLAI case for January in the Hadley cell upper branch maximum wind. There was also a slight (approximately 2%) increase in the maximum magnitude of the Hadley cell inflow from the Northern Hemisphere. However, maximum mass flux in the winter hemisphere Hadley cell was approximately 2% smaller in the actLAI case than in the potLAI case. The Northern Hemisphere Ferrell cell maximum mass flux was larger in the actLAI case than the potLAI case by approximately 20% (45×10^9 g/s as compared to 37×10^9 g/s).

The zonally-averaged vertical motion field (Figures 3.7) showed slight changes between cases in the January tropics and larger differences at higher latitudes. Peak rising motion at about 5°S is less deep in the actLAI case than the potLAI case, with the 0.03 Pa/s contour reaching to approximately 300 mb in the potLAI case while in the actLAI case this contour reached only 400 mb. The peak in upward motion was also nearly 3 degrees (1 grid interval) farther equatorward in the actLAI case as compared to the potLAI case. This shift in vertical motion was reflected in the northward movement in the precipitation maximum (Figure 3.4). The maximum vertical velocity near 10°S is decreased by about 4% in the actLAI case. Also of interest is a large (18%) decrease in maximum lower tropospheric upward motion

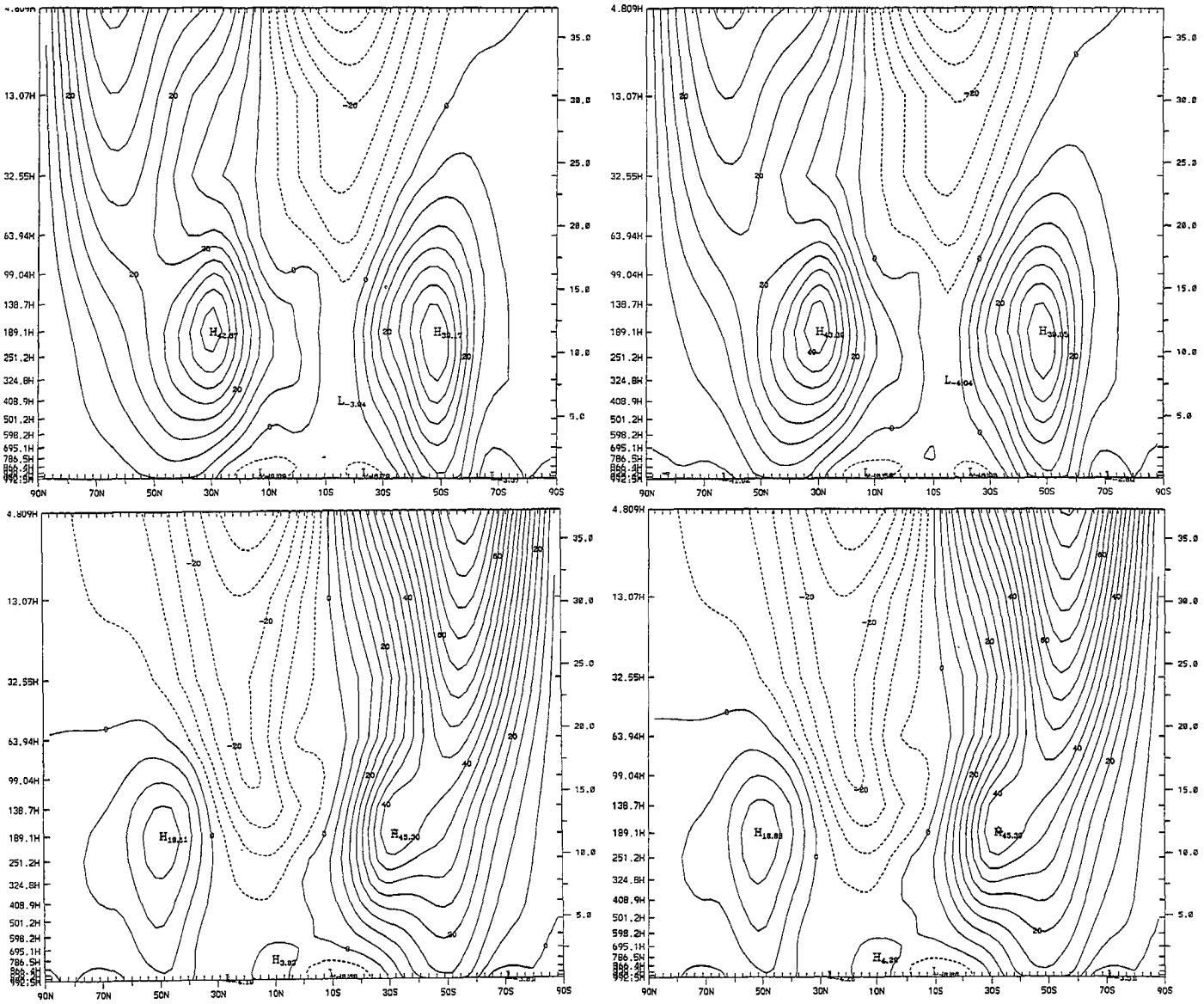

Figure 3.5: Zonally averaged zonal winds in m/s for a) January - actLAI, b) January - potLAI, c) July - actLAI, and d) July - potLAI.

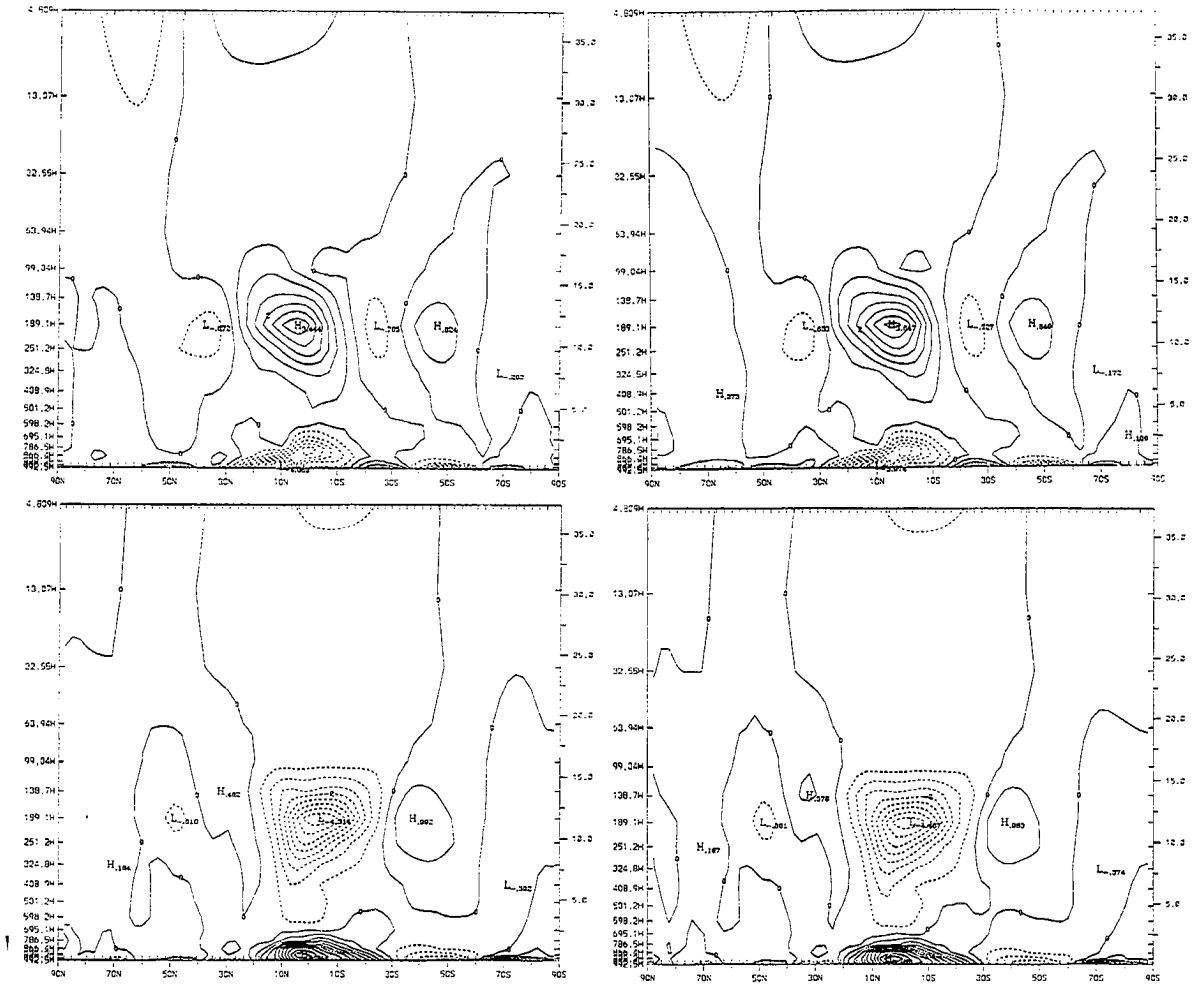

Figure 3.6: Zonally averaged meridional winds in m/s for a) January - actLAI, b) January - potLAI, c) July - actLAI, and d) July - potLAI.

from 50-60°N in the actLAI case. Upward motion was also more shallow in this region reaching 525 mb in the actLAI case as opposed to 400 mb in the potLAI case. In July, tropical maximum vertical motion in the actLAI case was slightly stronger than in the potLAI case but shallower and shifted more equatorward.

July maximum Hadley cell meridional winds were slightly stronger in the upper branch in the actLAI case as compared to the potLAI case though weaker in the lower branch. Despite this, the Southern Hemisphere Hadley circulation showed more than a 2% decrease in maximum mass flux in the actLAI case as compared to the potLAI case indicating that the stronger winds occur over a smaller area. The Northern Hemisphere Hadley cell mass flux decreased by nearly 15% in the actLAI case.

3.4 Meridional Averages

In order to better understand mechanisms responsible for the less vigorous Hadley circulations and zonal jets in both January and July in the actLAI simulation, surface quantities for each season were averaged over the latitude band which corresponded to the area of mean tropical ascending motion. For January this belt lies approximately from 2°N to 22°S. In July, the averaging area was from 2°N to 22°N.

Table 3.3 summarizes mean quantities over land in the latitude bands corresponding to mean upward motion for both January and July. There was a slightly larger average decrease in LAI in the actLAI case in January than in July and differences in surface fluxes in January were more than double the July values. The actLAI case showed increased sensible heat flux, decreased latent heat flux, and decreased precipitation on average in both seasons as compared to the potLAI case. Skin temperatures in the actLAI case increased in January but not in July. Outgoing Longwave Radiation (OLR) values for the actLAI case increased on average in

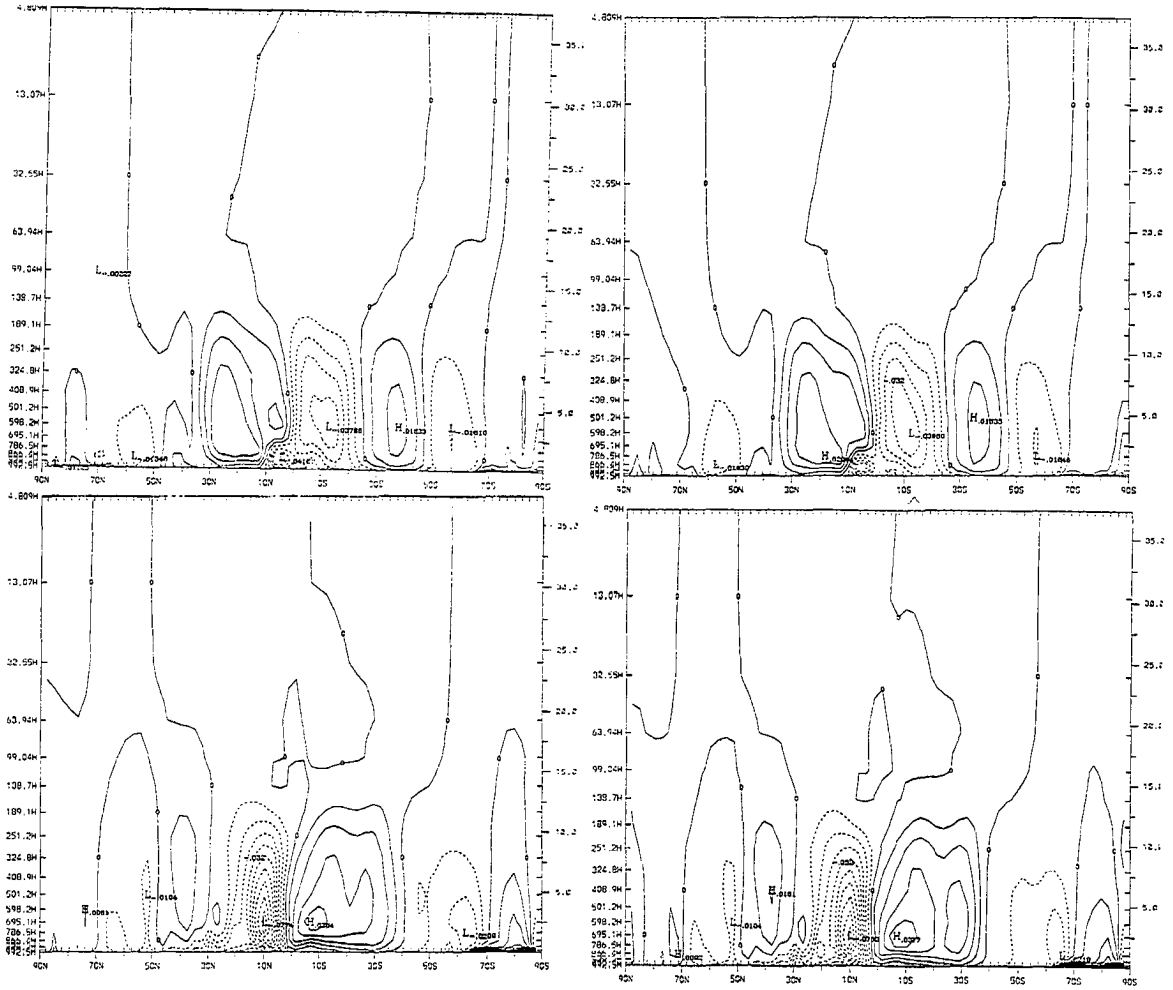

Figure 3.7: Zonally averaged pressure velocity in mb/s for a) January - actLAI, b) January - potLAI, c) July - actLAI, and d) July - potLAI.

VARIABLE	*JANUARY*	*JULY*
LEAF AREA INDEX	–0.7	–0.6
SENSIBLE HEAT FLUX (W/m^2)	+2.4	+1.1
LATENT HEAT FLUX (W/m^2)	–2.6	–1.0
SKIN TEMPERATURE (K)	+0.17	–0.05
OUTGOING LONGWAVE RADIATION (W/m^2)	1.3	–1.0
TOTAL PRECIPITATION (mm/day)	–0.09	–0.34

Table 3.3: Average differences over land surfaces (actLAI - potLAI) for tropical latitudes corresponding to mean upward motion. January (2°N–22°S) and July (2°N–22°N).

January but decreased in July. However, the largest change in total precipitation occurred in July.

Figures 3.8 and 3.9 show differences in surface quantities between cases in these same latitude belts. Maximum averaged differences in LAI between the two cases in these latitude bands were 1.8 in July as opposed to 1.5 in January (the maximum value of LAI in the model is 6). In January (Figure 3.8a), the largest differences occurred in Africa followed closely by the Americas, and were smallest in Asia in January. Note that in January, the averaging domain extends only to 2°N so that the main land masses of Asia are not included in the domain. We use Asia here for convenience in referring to Indonesia and the Maritime Continent. July LAI (Figure 3.9a) differences were largest in Asia and followed by the Americas and were relatively small in magnitude and area in Africa.

In January, (Figure 3.9a) difference fields comparing surface latent heat flux from 2°N–22°S showed decreased latent heat flux over land in the actLAI case with a maximum decrease of 12 W/m^2 occurring in the Americas. Decreases of about 8–10 W/m^2 covered most of Africa. A sharp increase of approximately 11 W/m^2 occurred in western Asia, while a decrease in latent heat flux of about 4 W/m^2 occurred in eastern Asia. This latter area was a region of small changes in LAI. Differences in sensible heating patterns occurred almost exclusively in regions affected by a change

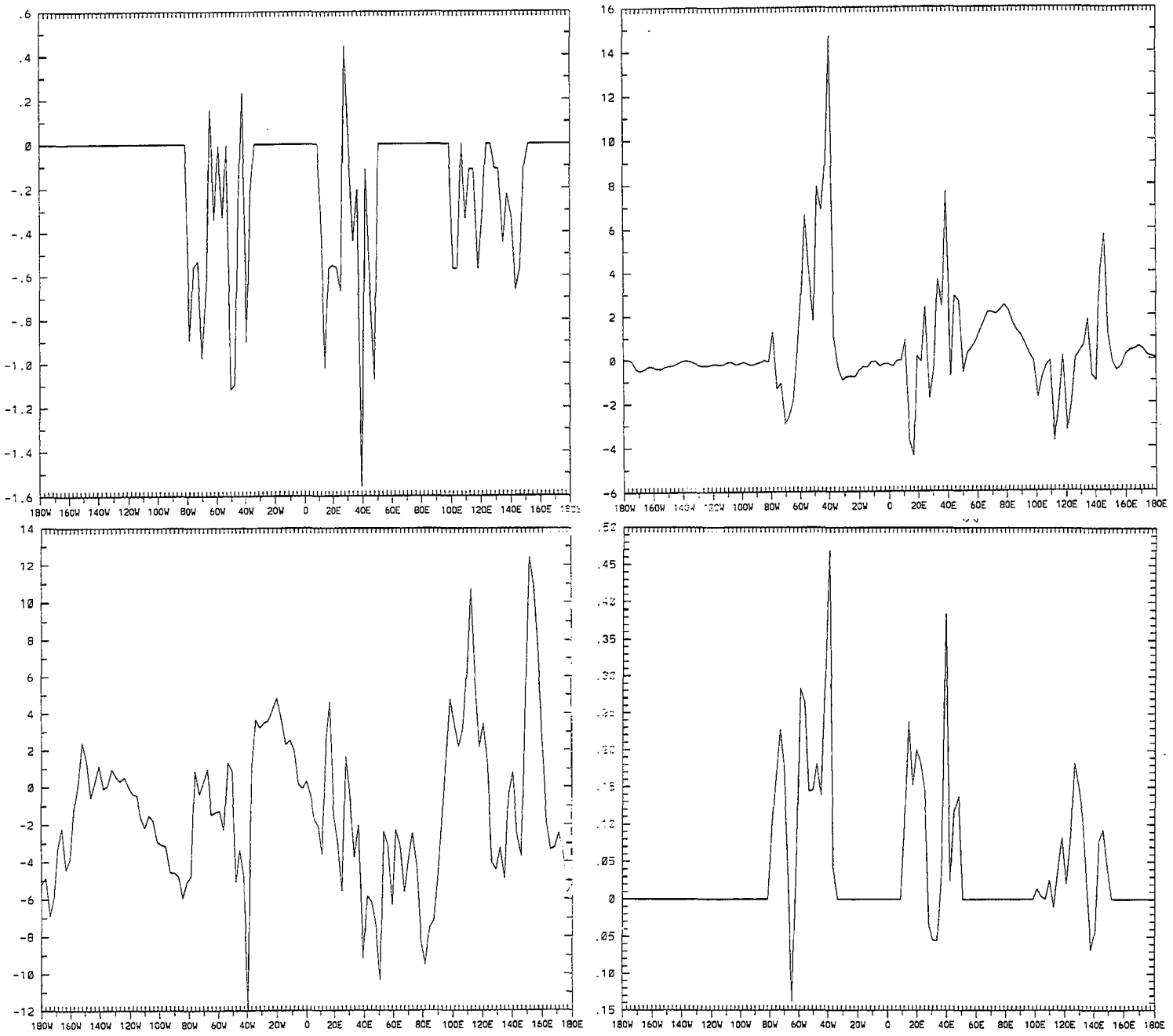

Figure 3.8: January mean (from 2N-22S) surface field differences (actLAI - potLAI). Differences in a) LAI, b) sensible heat flux from the surface (W/m^2), c) latent heat flux from the surface (W/m^2), and d) surface temperature (K).

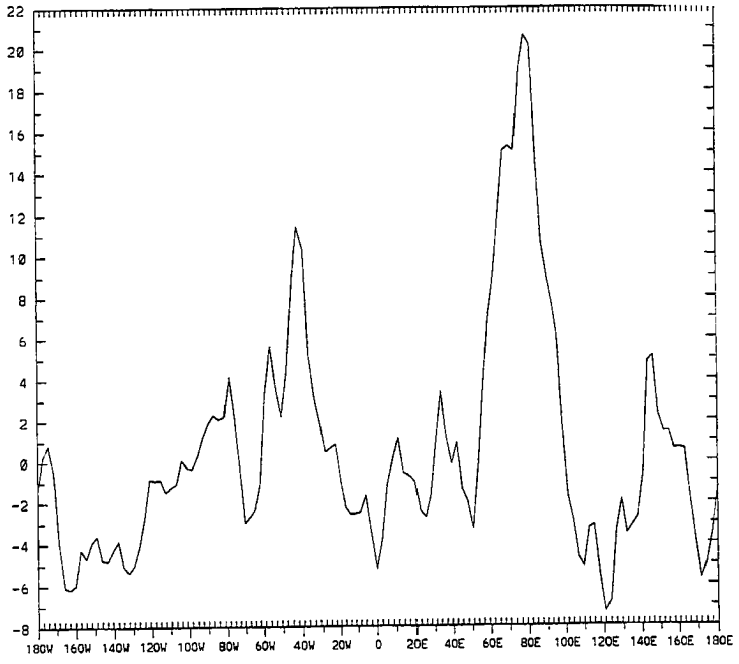

Figure 3.8: Continued. January mean (from 2N-22S) surface field differences (act-LAI - potLAI). Differences in e) outgoing longwave radiation.

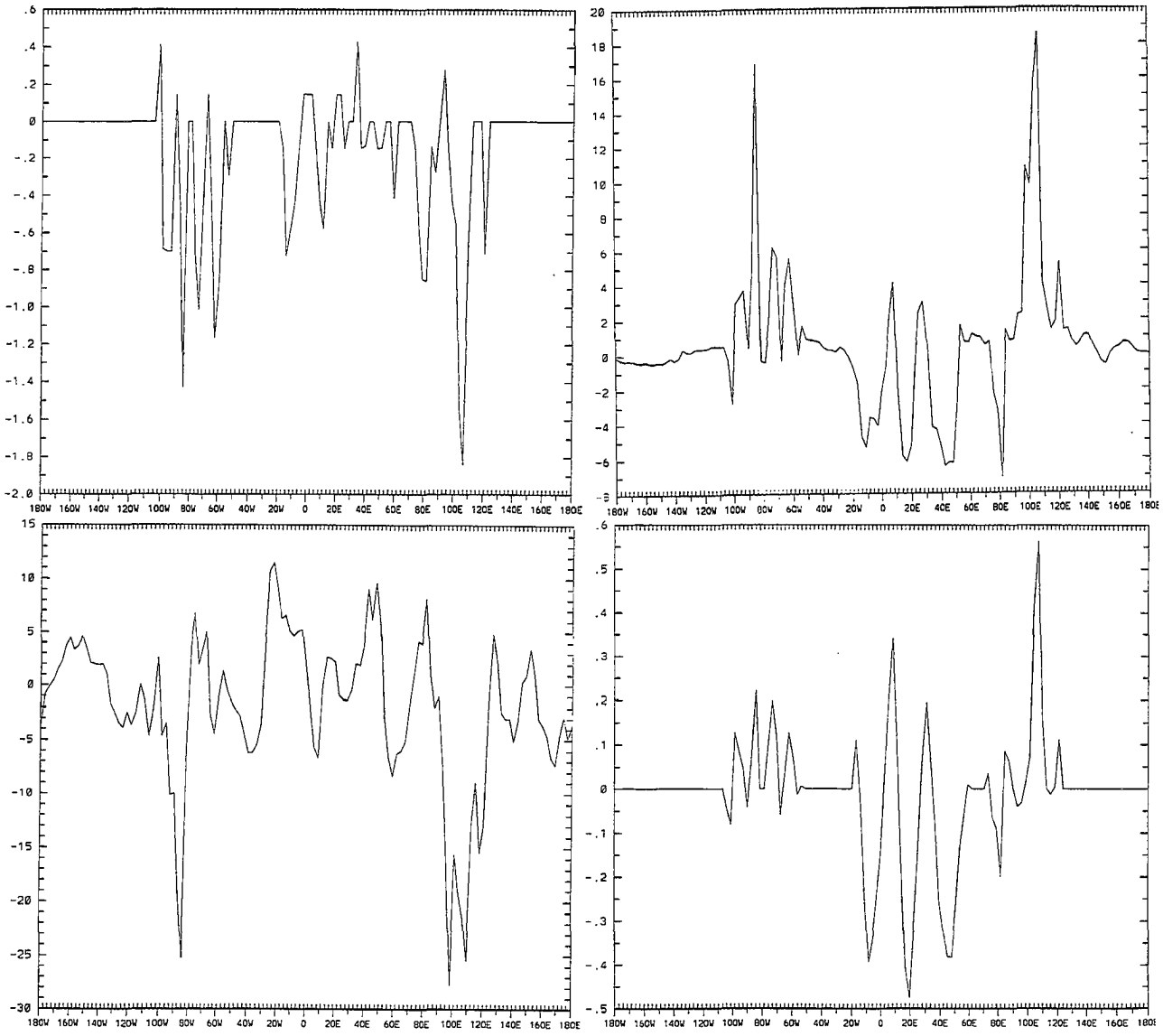

Figure 3.9: July mean (from 2N-22N) surface field differences (actLAI - potLAI). Differences in a) LAI, b) sensible heat flux from the surface (W/m^2), c) latent heat flux from the surface (W/m^2), and d) surface temperature.

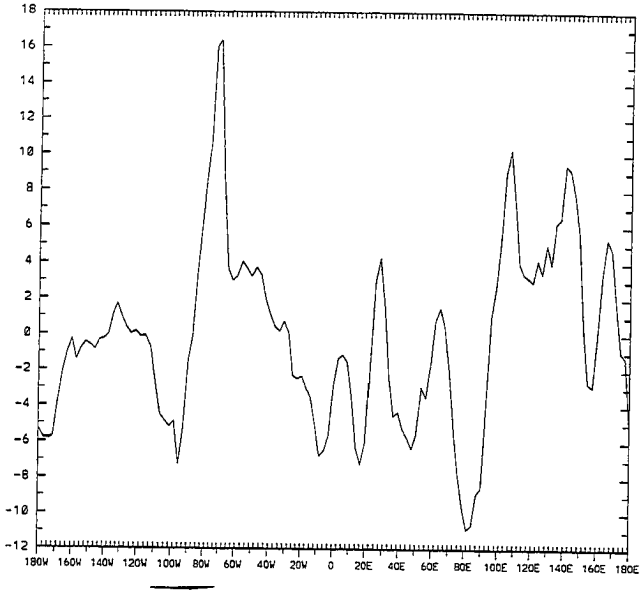

Figure 3.9: Continued. July mean (from 2N-22N) surface field differences (actLAI - potLAI). Differences in e) outgoing longwave radiation.

in LAI. Areas of increased sensible heating occurred on nearly all land areas in the averaging domain with a maximum increase of nearly 15 W/m^2 in the Americas for the actLAI case.

An estimate of the vigor of convection in the tropics is outgoing longwave radiation (OLR) with OLR decreasing with deeper convection. In January, OLR increases in the actLAI case over the Americas reached 12 W/m^2. Off the eastern coast of Africa in the Indian Ocean, increases in the actLAI case were in excess of 20 W/m^2 and over eastern Asia, OLR increased 5 W/m^2. Over the eastern Pacific, the Atlantic and Africa OLR decreased in the actLAI case indicating increased convective activity in these regions.

In July, (Figure 3.9) decreases in mean latent heat flux in the latitudes from 2°N–22°N for the actLAI case were largest in Asia which corresponds to the region of largest decrease in LAI. The maximum decrease was nearly 30 W/m^2 for the actLAI case. A decrease of 25 W/m^2 developed in the Americas. For the same case, increases in sensible heating occurred in the Americas and Asia in direct correlation with decreases in latent heat flux. The largest increase was nearly 19 W/m^2 in Asia.

OLR increases of up to 16 W/m^2 occurred over the Americas in the actLAI case in July. Over Africa, OLR decreased in this case to 8 W/m^2. Over Asia and the maritime continent OLR increased by up to 11 W/m^2.

In order to identify any changes to the longitudinal structure of the winter hemisphere zonal jet due to altered heating patterns in the tropics, averages of the zonal winds in the latitude belts from 10N-40N in January and 10S-40S in July were taken. Local changes in the jet maxima do occur and are possibly associated with the greater latent heating over land surfaces. The January 200 mb jet (Figure 3.10) maximum winds over the Americas decrease from 35.5m/s to 30 m/s. The jet core in this case is also less confined in the east-west direction than in the potLAI case. Over Africa the jet core has strengthened from 37.2 m/s in the potLAI case to 40.2

m/s in the actLAI case. Over Asia it has weakened slightly. Easterlies at the surface show marked increase in the actLAI case. Difference fields of the zonal velocity in this belt show increased westerlies globally for the potLAI case everywhere except in the longitudes from approximately 0–60E where velocities decrease all through the atmosphere.

The southern hemisphere zonal jets in July averaged from 10S–40S show insignificant differences between the cases than in January. Such small differences despite relatively large changes in heating patterns in July may be a reflection of the generally smaller gradients of temperature and weaker jet in the winter hemisphere. The difference field for July zonal winds again shows increased westerlies from 120E to 60W moving westerly while decreased westerlies occur from 60W to 120E.

It should be emphasized that the differences described in this section were small in the sense that differences between cases were smaller than the year-to-year variability of the fields in the model.

3.5 Deviations from the Mean

Figure 3.11 displays comparisons of the horizontal momentum fluxes representing deviations from the zonal mean flow averaged vertically from 1000 to 100 mb. Northward momentum flux associated with stationary waves in January was somewhat larger in magnitude in the actLAI case than for the potLAI case in the Northern Hemisphere. There was, however, a considerable decrease in southerly momentum transport poleward of 50°N in the actLAI case creating a decrease in zonal momentum convergence and shifting the area of convergence farther north. Fluxes of temperature by standing eddys are quite similar in magnitude in the two cases though the peak in transport of temperature has moved slightly southward in the potLAI case.

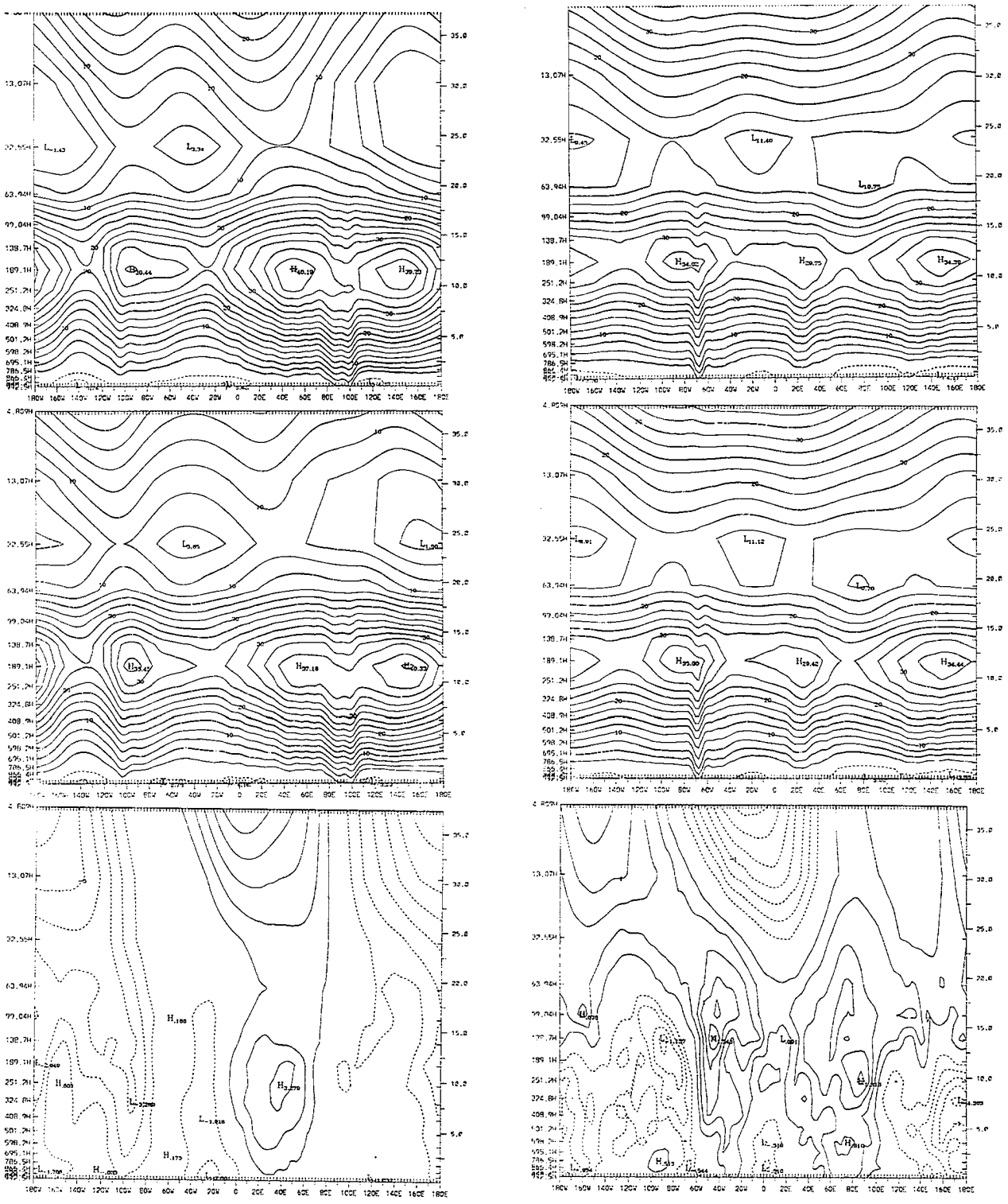

Figure 3.10: January and July, meridionally averaged from 10N-40N, 10S-40S respectively zonal winds (m/s) a) January - actLAI, b) July - actLAI, c) January - potLAI, d) July - potLAI, e) January difference (actLAI-potLAI), and f) July differenct (actLAI-potLAI).

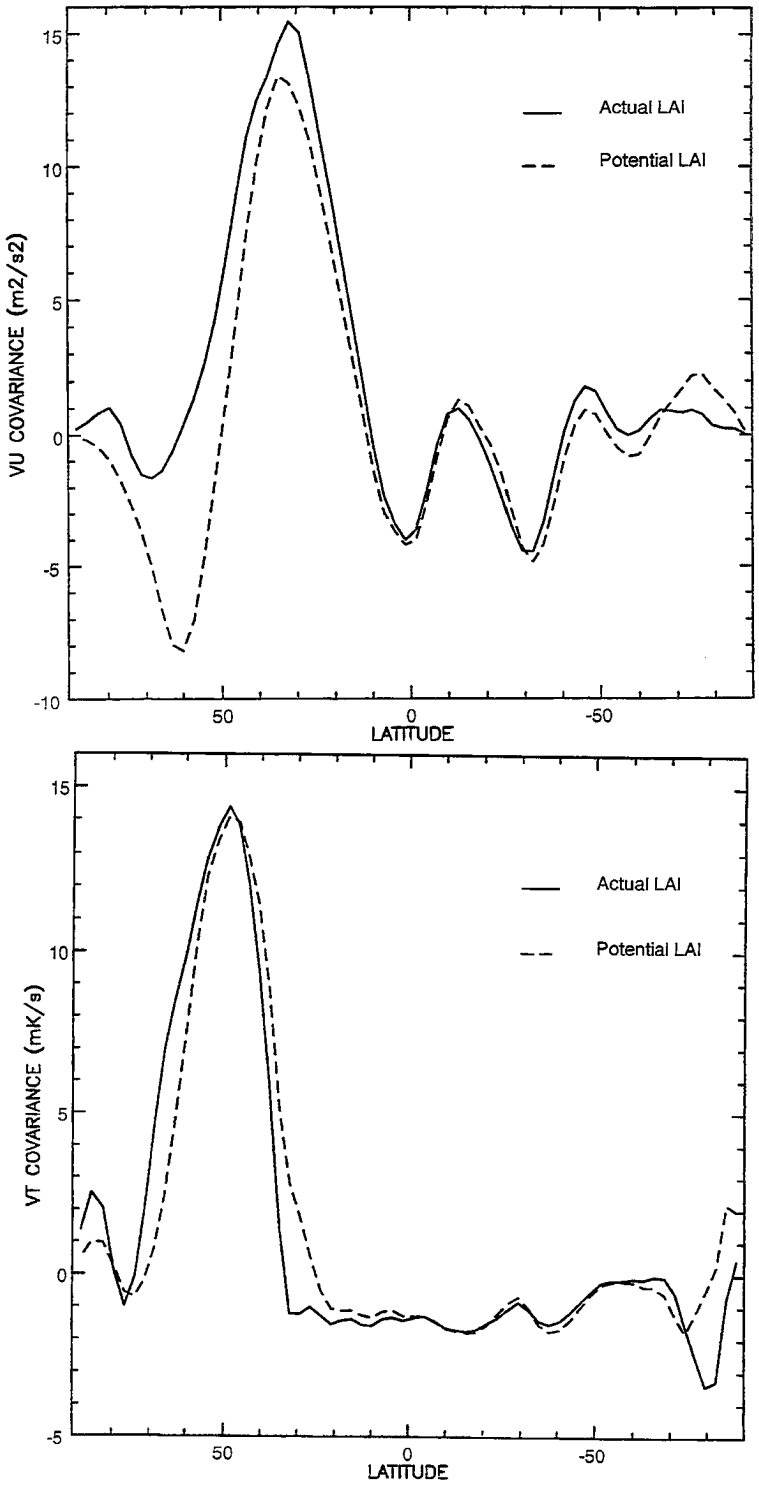

Figure 3.11: Vertically averaged standing eddy fluxes a) $\left[\overline{V*U*}\right]$ January, and b) $\left[\overline{V*T*}\right]$ January.

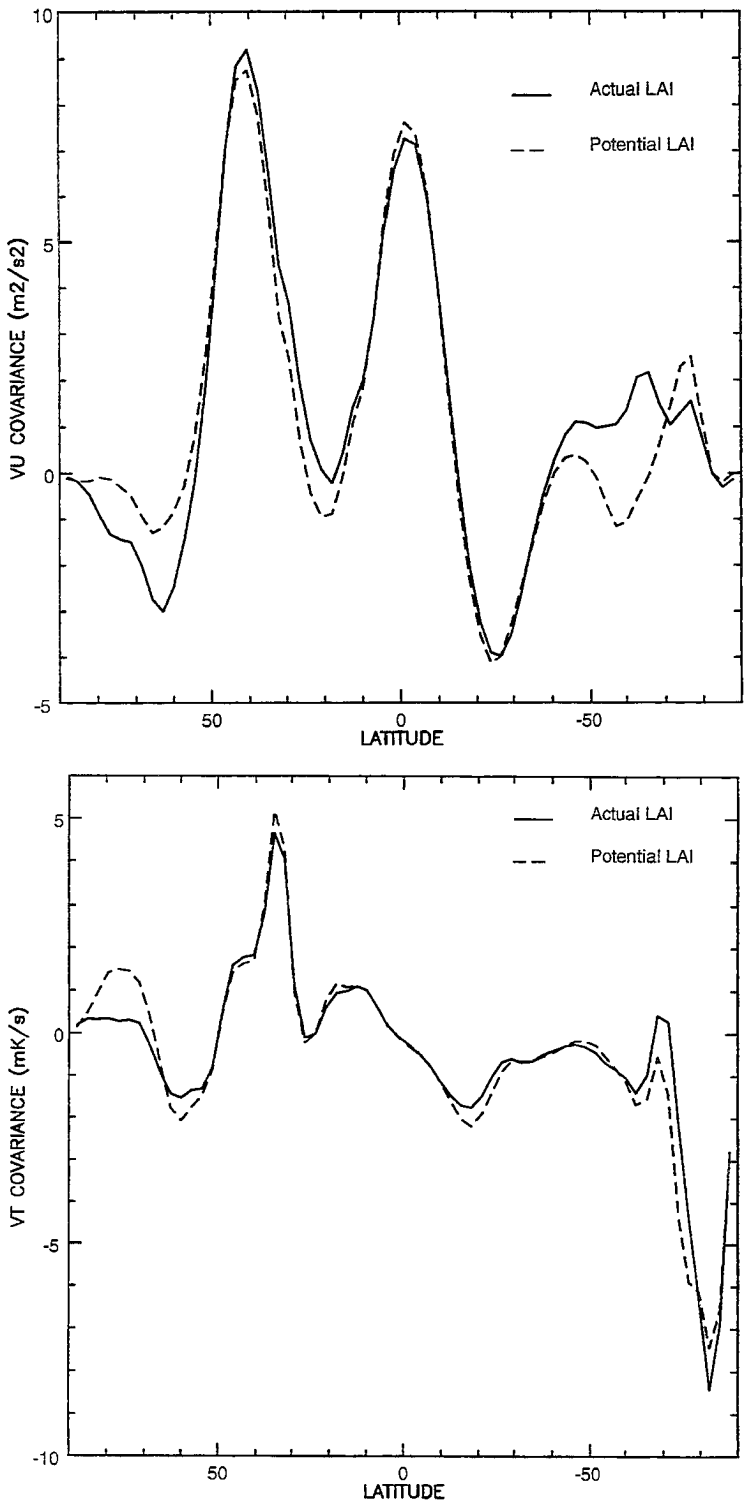

Figure 3.11: Continued. Vertically averaged standing eddy fluxes c) $\left[\overline{V * U*}\right]$ July, and d) $\left[\overline{V * T*}\right]$ July.

In July, the Northern Hemisphere standing wave fluxes were similar in the two cases though the actLAI case had slightly smaller magnitude in far northern latitudes. Larger differences in the flux patterns were seen in the Southern Hemisphere. The actLAI case had larger magnitude zonal momentum fluxes which were consistently positive in the Southern Hemisphere poleward of 40°S while momentum fluxes for the potLAI case in the Southern Hemisphere were negative until about 70°S. The temperature flux plots show smaller negative values of temperature fluxes in the Southern Hemisphere equatorward of 70S in the actLAI case.

Fluxes representing deviations from the time mean also displayed interesting differences between the two experiments. Differences between the vertically-averaged (1000–100 mb), zonally-averaged transient fluxes are shown in Figure 3.12. In January, transient eddy fluxes of zonal momentum are larger in magnitude for the actLAI case between 55°N and 70°N. Between 30°N and 55°N transient transport of zonal momentum was considerably smaller for the actLAI simulation. The decrease in transient flux in this region in the actLAI case was associated with a northern mid-latitude decrease in precipitation (Figure 4). Again, there was less convergence of zonal momentum at about 60°N for the actLAI case. This decrease in zonal momentum convergence presumably served to decrease the magnitude of the jet, thereby increasing its stability, and so further reduced transport by transient eddies. There is a considerably smaller magnitude northerly flux of temperature from about 50N - 70N in the actLAI case while south of this the temperature flux differences between the two cases are quite small.

In July, transient activity was generally smaller in magnitude in the northern mid-latitudes for the actLAI case. Transient eddy momentum flux was larger in magnitude for the actLAI case in most of the Southern Hemisphere. Temperature flux differences are very similar in pattern and magnitude for both cases.

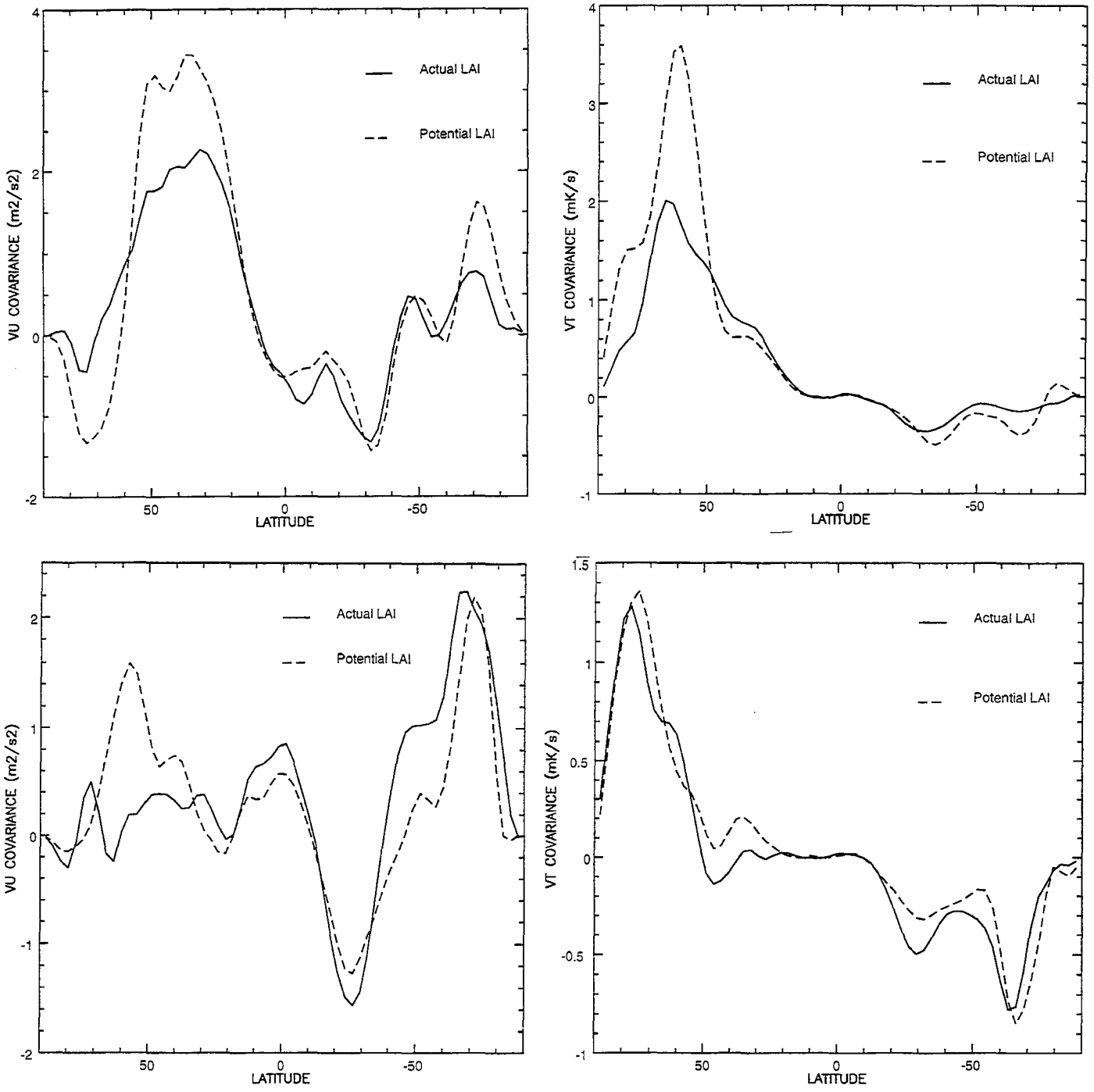

Figure 3.12: Vertically averaged transient eddy fluxes for a) $V'U'$ January, b) $V'T'$ January , c) $V'U'$ July, and d) $V'T'$ July.

3.6 Interannual Variability

As an example of the differences in variability between the the two simulations, Figure 3.13 compares the variance of 500 mb heights for the two experiments. In the regions poleward of the polar front, the variance of the actLAI fields was substantially smaller in both seasons and for both hemispheres. The decrease in variance for the actLAI case was nearly 40% at the peak in January. In July, the peak variance in the Southern Hemisphere also shifted equatorward approximately 15 degrees in the actLAI case.

3.7 Asian Monsoon

A closer look at southern Asia during northern summer is interesting for several reasons. First, this region was subject to relatively large increases in LAI over a large continuous area. Also, these changes were from large values (potLAI) to small values (actLAI). If LAI differences resulted in changed atmospheric conditions, then it should be noticeable here. Second, there is much interest in the influence of the land surface on the strength of the Asian summer monsoon (e.g., Meehl, 1993, 1994; Fennessey et al., 1994).

Ten years of July averages have been used to represent the summer monsoon season. Though this is not ideal it was felt that this would be somewhat representative of the summer monsoon season as a whole. A summary of regionally-averaged differences over land surfaces from 10°S-35°N and 65-130°E are presented in Table 3.4. In this region, the actLAI case had more than a 20% decrease in LAI on average compared to the potLAI case. As a consequence there was an decrease in latent heat flux from the surface of 133.2 W/m^2 to 126.8 W/m^2. Sensible heat fluxes increased from 47.6 W/m^2 to 53.4 W/m^2. This was followed by a 0.3 K increase in 1.5 m temperatures for the actLAI case. A 0.5 K increase in maximum daily temperature occurred in this region, while minimum daily temperature decreased 0.3 K. The

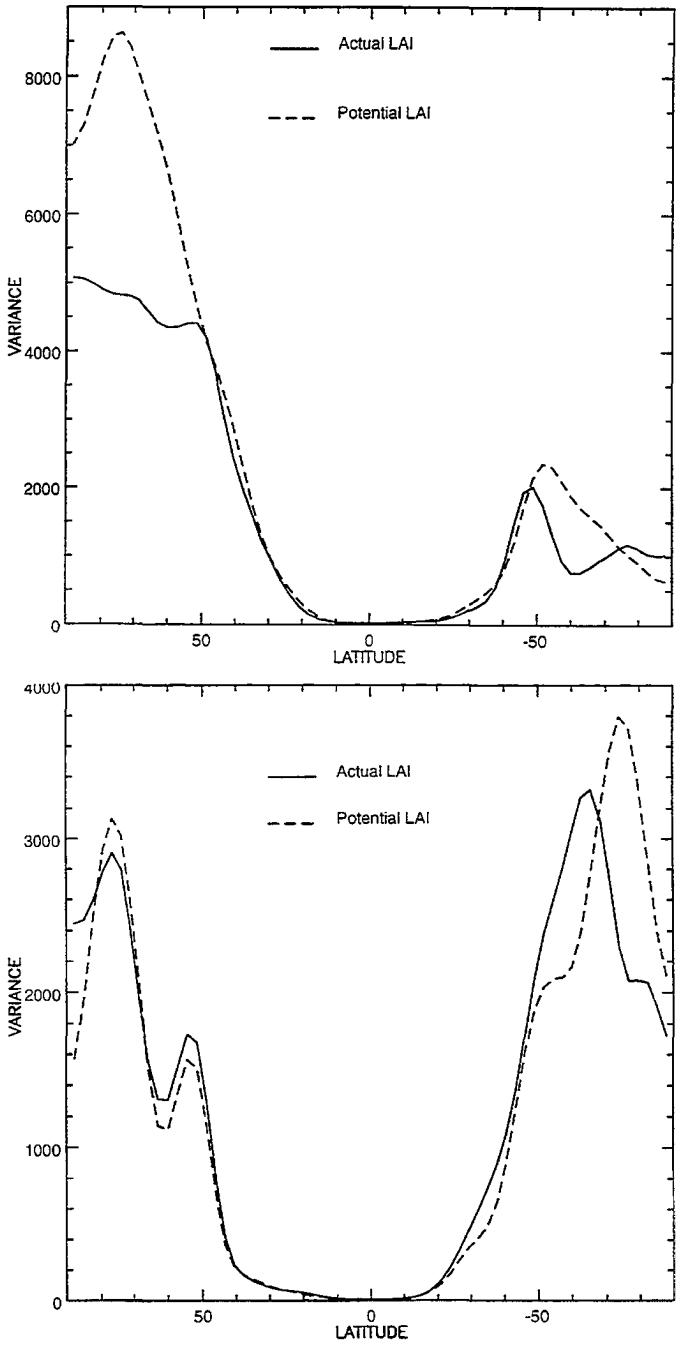

Figure 3.13: Zonally averaged variance differences for a) January 500 mb heights, and b) July 500 mb heights.

increased vegetation increased the diurnal temperature range. A decrease in total precipitation in the actLAI case occurred over land surfaces from 12.5 mm/day to 11.8 mm/day in this region. July precipitation decreases over land occurred largely over Nepal and Tibet, southeast Asia, and the northern Philippines (Figure 3.14). Increased precipitation occurred over southern India.

VARIABLE	*JULY*	*% CHANGE*
Leaf Area Index	-1.38	-20.8%
Total Soil Moisture (mm)	-0.12	-
Skin Temperature (K)	+0.40	-
Maximum 1.5 m Temperature (K)	+0.54	-
Minimum 1.5 m Temperature (K)	-0.34	-
Average 1.5 m Temperature (K)	+0.29	-
Sensible Heat Flux (W/m^2)	+5.8	+12.1%
Latent Heat Flux (W/m^2)	-6.4	-4.8%
Total Clouds (frac)	+0.02	+2.4%
Total Precipitation (mm/day)	-0.66	-5.2%
Runoff (mm/day)	-0.46	-6.3%
Short Wave at Surface (W/m^2)	+3.43	-

Table 3.4: July land averages (65-130°E, 10S-35°N). Summary of differences between control and perturbed (actLAI - potLAI) and the percentage change. A dash indicates less than 1% change.

3.8 Statistical Significance

Statistical significance of results from this experiment was estimated using the methodology described in Chervin and Schneider (1976) based on the t-test statistic. Figure 3.15 displays contoured values of this statistic at the 80% (t = 1.33), 90% (1.73), 95% (2.10) and 98% (2.55) significance levels for the 500 mb height field in January and July. The areas along the storm tracks in the Northern Hemisphere in January clearly showed regions of significant difference between the two experiments. In the zonal average, the t-statistic was greater than the 80% significance level for

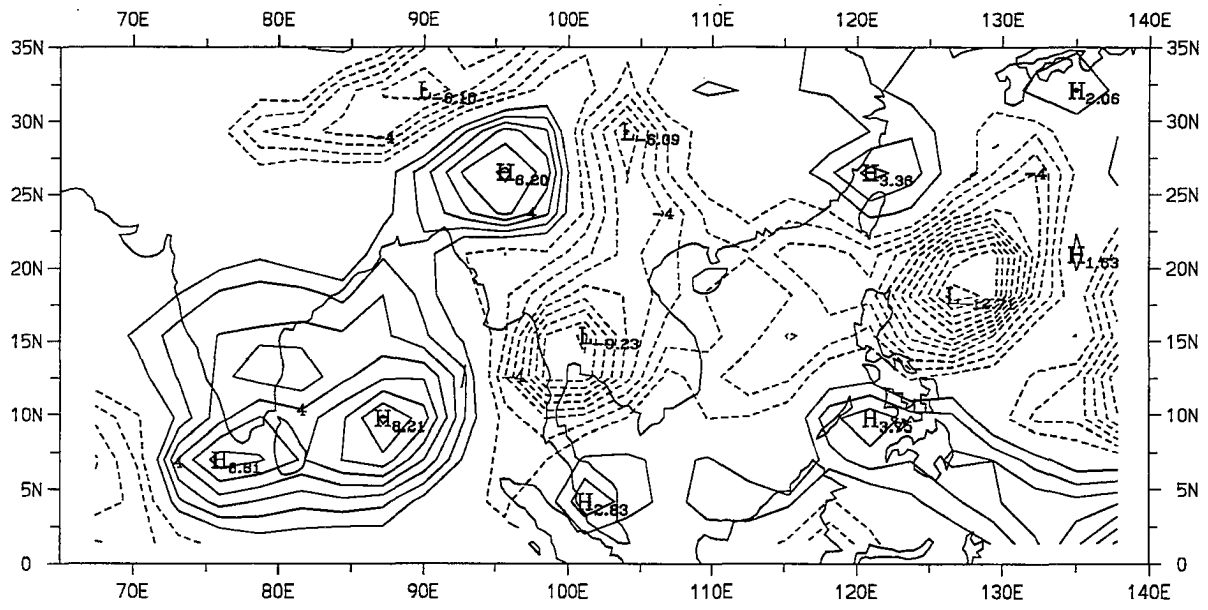

Figure 3.14: Total precipitation differences (actLAI-potLAI) in the region from 65-130E, 10S-35N in July.

most of the Northern Hemisphere north of 60°N. In July, the region of highest significance was the tropics where greater than 90% significance level was reached from approximately 5°N to 10°S. The zonally-averaged planetary circulation shows differences between experiments but these differences tend to be smaller than model variability. Regions of 80% or higher significance exist but are isolated so that significant levels are smoothed out in the zonal average and therefore are statistically unreliable.

Because statistical tests are not conclusive, comparisons between the first five-year and the second five-year means have been made in order to test the consistency of results in separate subsets. Both five-year samples show differences along the winter hemisphere polar front which can be ascribed to altered wave patterns. Moreover, the differences in pattern are very similar in each five-year mean indicating that a constant rather than random perturbation is responsible. Both five-year averages show decreased latent heat flux in the tropics, weaker Hadley circulations, and broader, slower jets in January in the actLAI case. Both five-year averages show decreased variability in the actLAI case and decreased convergence of zonal momentum in January in the Northern Hemisphere. Results from the Asian monsoon region are also consistent between the two five-year samples with an overall decrease in precipitation over land, a warming of the surface, decreased latent heat flux and increased sensible heat flux in the actLAI case.

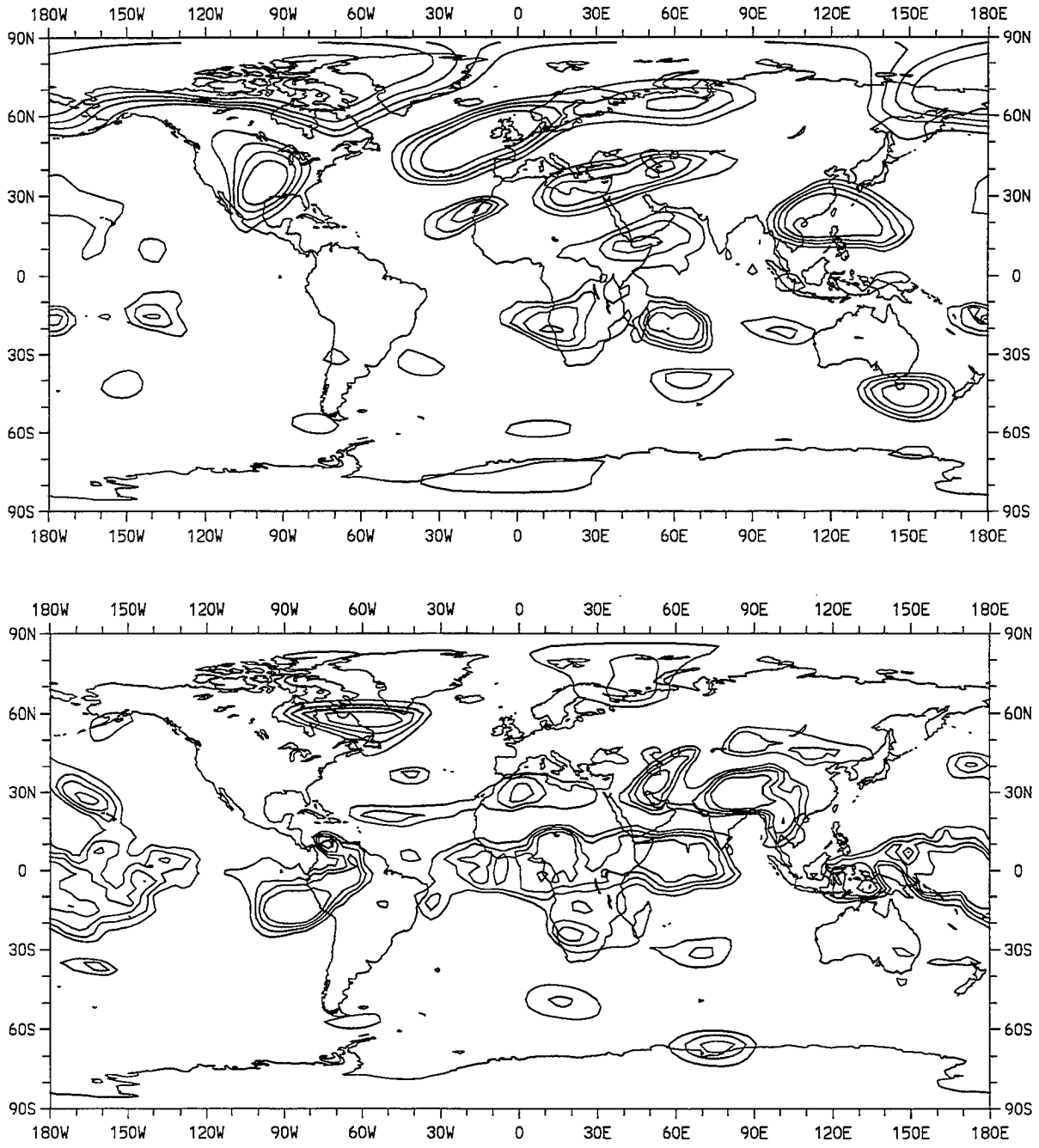

Figure 3.15: t-Statistic. a) January 500 mb heights and b) July 500 mb heights. Contours are the 80, 90, 95, 98% significance levels.

Chapter 4

DISCUSSION AND CONCLUSIONS

An experiment designed to test the sensitivity of numerically modeled climate to a change in maximum leaf area index using a plausible perturbation was performed. This change is the difference between a global distribution of maximum LAI observed from satellite and an estimate of the distribution of maximum LAI modeled to be in equilibrium with current observed climate.

Globally-averaged fields in these experiments showed few differences. The changing distribution and magnitude of LAI would be expected to initially alter only the partitioning between latent and sensible heat fluxes from the surface. While differences in this partitioning may possibly have large consequences regionally due to altered circulation patterns it is unlikely that changes would be seen in globally-averaged and time-averaged fields. An exception to this would occur if cloud cover were altered or changes in soil moisture were induced by the LAI change. Both these factors affect global albedo and therefore the planetary energy budget (e.g., Ramanathan et al. 1989; Otterman, 1977). Because differences in both total cloudiness and soil moisture were negligible in the global average, there is no reason to expect that these will play anything but a small role in this experiment in terms of global-mean effects. However, large-scale features in the atmosphere were affected by the change from the potential LAI distribution to the actual LAI distribution in the simulations. This was seen in higher latitudes in winter in both hemispheres, as well as in the tropics.

Statistically significant differences at high northern latitudes in January seen in 1.5 m temperatures or the 500 mb heights are attributed to changes in the structure of waves along the polar front. It is inferred that these differences were generated by changes in atmospheric heating patterns in the tropics initiated by decreased average latent heat flux from the surface in the actual LAI simulation and from changes in the meridional distribution of heating. These changes in tropical heating patterns appear to have altered the meridional structure in the 200 mb jet and so the generation of waves. This was evident in January in the region of the Americas where the jet shows a 14% decrease in peak magnitude. While regional differences in latent heat flux were larger in the July tropics, there was less of an effect at higher latitudes in the Southern Hemisphere. This would seem to be due to the greater role eddies have in the Northern Hemisphere because of the larger percentage of land surface.

Differences between the actual LAI simulation and the potential LAI simulation were also found in the tropics at the latitudes of maximum upward motion. While scattered areas of greater than 90% statistical significance occurred in this region, the significance of the results throughout the tropics and higher latitudes is not fully established. However, these differences were often consistent in comparisons of two five-year samples. This suggests that a longer integration would differentiate a similar signal as described here from model noise. There was an decrease of surface latent heat flux and increased sensible heat flux over land in both January and July due to the decreased LAI in the actLAI case. The decreased latent heat flux surpassed the increased sensible heat flux in absolute value in both seasons so that the surface was supplying less total energy to the atmosphere on average. A small decrease in total precipitation was seen in the tropical latitudes of interest in both seasons. Decreased precipitation and increased OLR in January indicates weaker tropical convection in this season. This may explain the small decrease

in magnitude of the Hadley cell mass flux and in the magnitude of the 200 mb Northern Hemisphere jet in January. Despite the decreased precipitation in July in the tropical latitude belt of ascending motion, OLR decreases in July indicate an increase in convective activity. This contradiction emphasizes the weakness of the signal due to altered LAI relative to other processes at work. The mean meridional circulation and the winter hemisphere jet were also slightly weaker in this season.

The region of the Asian monsoon in July displayed a similar response to the decrease in LAI in the actual LAI case as the tropics as a whole. There was decreased latent heat flux over land, increased sensible heat flux, and an decrease in total precipitation.

The most striking differences between the two cases described here occurred in the realm of interannual variability and eddy fluxes. There was decreased variability in the actual LAI simulation along and poleward of the winter hemisphere polar fronts which again point to alterations in the generation of waves due to influences from the tropics.

Finally, it should be emphasized that this was a minimal change scenario designed to test the sensitivity of the model to perturbation in LAI. Interactions among biophysical changes associated with altered vegetation structure are needed to consider the effect of vegetation as a whole on climate. Future work should include time varying roughness length, vegetation albedos, vegetation fraction, and other parameters used to describe the vegetation cover which are compatible with the LAI distribution. Further, because neither vegetation fraction nor minimum LAI were altered along with the maximum LAI, this experiment may be considered to have evaluated minimal forcing arising from changes in LAI. Presumably the decreased density of vegetation seen in the actual LAI distribution in most areas also covered smaller fractional areas of the surface and so effects due to LAI changes would be proportionally larger. Nonetheless, the designation of LAI as part of the bottom

boundary condition in this model appears to have had an effect on the climate generated suggesting that further attention to the accurate specification of vegetation density is necessary.

REFERENCES

Bonan, G.B., D. Pollard, and S.L. Thompson, 1992: Effects of boreal forest vegetation on global climate. *Nature*, **359**, 716.

Bonan, G.B., D. Pollard, and S.L. Thompson, 1993: Influence of sub-grid scale heterogeneity in leaf area index, stomatal resistance, and soil moisture on grid-scale land-atmosphere interactions. *J. Climate*, **6**, 1882-1897.

Briegleb, B.P., 1992: Delta-Eddington approximation for solar radiation in the NCAR Community Climate Model. *J. Geophys. Res.*, **97**, 7603-7612.

Charney, J.G., 1975: Drought in the Sahara: A biogeophysical feedback mechanism. *Science*, *187*, 434-435.

Collins, D.C., and R. Avissar, 1994: An evaluation with the Fourier amplitude sensitivity test of which land-surface parameters are of greatest importance in atmospheric modeling. *J. Climate*, **7**, 681-703.

Denmead, O.T. and B.D. Miller, 1976: Field studies of the conductance of wheat leaves and transpiration. *Agron. J.*, **68**, 307-311.

Fennessey, M.J., J.L. Kinter, B. Kirtman, L. Marx, S. Nigam, E. Schneider, J. Shukla, D. Straus, A. Vernekar, Y. Xue, and J. Zhou, 1994: The simulated Indian monsoon: A GCM sensitivity study. *J. Climate*, **7**, 33-43.

Gamon, J.A., G.C. Bield, M.L. Goulden, K.I. Griffin, A.E. Hartley, G. Joel, J. Penuelas, and R. Valentini, 1995: Relationships between NDVI, canopy struc-

ture, and photosynthesis in three California vegetation types. *Ecol. Appl.*, **5**, 28-41.

Garratt, J.R., 1992: Sensitivity of climate simulations to land-surface and atmospheric boundary-layer treatments - A review. *J. Climate*, **6**, 419-449.

Gill, A.E., 1980: Some simple solutions for heat-induced tropical circulations. *Quart. J. Roy. Meteor. Soc.*, **106**, 447-462.

Gornitz, V., 1987: Climatic consequences of anthropogenic vegetation changes. In *Climate History, Periodicity and Predictability.* M.R. Rampino, J.E. Sanders, W.S. Newman, and L.K. Konigsson, Eds. Van Nostrand Reinhold Co. Inc., New York, 47-70.

Goward, S.N., C.J. Tucker, and D.G. Dye, 1986: North American vegetation patterns observed with the NOAA-7 Advanced Very High Resolution Radiometer. *Vegetatio*, **64**, 3-14.

Hack, J.J., 1994: Parameterizations of moist convection in the National Center for Atmospheric Research community climate model (CCM2). *J. Geophys. Res.*, **99**, 5551-5568.

Hack, J., B. Boville, B. Briegleb, J. Kiehl, P. Rasch, and D. Williamson, 1993: Description of the NCAR Community Climate Model (CCM2). NCAR Technical Note 382 + STR, 108 pp.

Henderson-Sellers, A.H., 1993: A factorial assessment of the sensitivity of the BATS land-surface parameterization scheme. *J. Climate*, **6**, 227-247.

Henderson-Sellers, A. and V. Gornitz, 1984: Possible climatic impacts of land cover transformations with particular emphasis on tropical deforestation. *Climatic Change*, **6**, 231-257.

Henderson-Sellers, A., and K. McGuffie, 1995: Global climate models and 'dynamic' vegetation. *Global Change Bio.*, **1**, 63-75.

Holtslag, A.A.M., and B.A. Boville, 1993: Local versus nonlocal boundary layer diffusion in a global climate model. *J. Climate*, **6**, 1825-1841.

Houghton, R.A., 1994: The worldwide extent of land-use change. *Bioscience*, **44**, 305-313.

Hoskins, B.J., and D.J. Karoly, 1981: The steady linear response of a spherical atmosphere to thermal and orographic forcing. *J. Atmos. Sci.*, **38**, 1179-1196.

Jacobs, C.M.J., and H.A.R. DeBruin, 1992: The sensitivity of regional transpiration to land-surface characteristics: Significance of feedbacks. *J. Climate*, **5**, 683-698.

Li, B., and R. Avissar, 1994: The impact of spatial variability of land - surface characteristics on land surface heat fluxes. *J. Climate*, **7**, 527-537.

Matthews, E., 1983: Global vegetation and land use: New high resolution data bases for climate studies. *J. Climate Appl. Meteor.*, **22**, 474-487.

Meehl, G.A., 1993: Influence of the land surface in the asian summer monsoon: external conditions versus internal feedbacks. *J. Climate*, **7**, 1033-1049.

Meehl, G.A. 1994: Coupled land-ocean-atmosphere processes and south Asian monsoon variability. *Science*, **266**, 263-267.

Meher-Homji, V.M., 1991: Probable Impact of deforestation on hydrological processes. *Climatic Change*, **19**, 163-173.

Mintz, Y., 1984: The sensitivity of numerically simulated climates to land-surface boundary conditions. *The Global Climate*, J. Houghton, Ed., 79-105.

Neilson, R., 1993: Vegetation redistribution: A possible source of CO_2 during climate change. *Water Air Soil Poll.*, **70**, 659-673.

Nemani, R.R., and S.W. Running, 1989: Testing a theoretical climate-soil-leaf area hydrologic equilibrium of forests using a satellite data and ecosystem simulation. *Agric. Forest Meteor.*, **44**, 245-260.

Nemani, R., S. Running, and R. Pielke, 1995: Influence of global vegetation cover changes on land surface temperature. *J. Geophys. Res.*, (submitted).

Otterman, J., 1977: Anthropogenic impact on the albedos of earth. *Climatic Change*, **1**, 137-155.

Overpeck, J.T., 1993: The role and response of continental vegetation in the global climate system. *Global Changes in the Perspective of the Past.* J.A. Eddy, and H. Oeschger, Eds., John Wiley and Sons Ltd.

Pielou, E.C., 1991: *After the Ice Age: The Return of Life to Glaciated North America.* The University of Chicago Press, Chicago and London, 366 pp.

Potter, Gerald L., H.W. Ellsaesser, M.C. MacCracken, and J.S. Ellis, 1981: Albedo change by man. *Nature*, **291**, 47-49.

Ramage, C.S., 1968: Role of a tropical "maritime continent" in the atmospheric circulation. *Mon. Wea. Rev.*, **96**, 365-370.

Ramanathan, V., R.D. Cess, E.F. Harrison, P. Minnis, B.R. Barkstrom, E. Ahmad, and D. Hartmann, 1989: Cloud-radiative forcing and climate: results from the earth radiation budget experiment. *Science*, **6**, 57-63.

Rasmusson, E.M., and K. Mo, 1993: Linkages between 200-mb tropical and extratropical circulation anomalies during the 1986-1989 ENSO cycle. *J. Climate*, **6**, 595-616.

Rowntree, P.R, 1988: Review of GCMs as a basis for predicting the effects of vegetation change on climate. In *Forests, Climate and Hydrology-Regional Impacts.* E.R.C. Reynolds, and F.B. Thompson, Eds., The United Nations University. p.162.

Sagan, C., O.B. Toon, and J.B. Pollack, 1979: Anthropogenic climate changes and the earth's climate. *Science*, **206**, 1363-1368.

Street-Perrott, F.A., J.F.B. Mitchell, and D.S. Marchand, 1990: Milankovich and albedo forcing of the tropical monsoons: A comparison of geological evidence and numerical simulations for 9000 y BP. *Trans R. Soc. Edin. Earth Sci.*, **81**, 407-427.

Sud, Y.C., and W.E. Smith, 1985: The influence of surface roughness of deserts on the July circulation. *Bound.-Layer Meteor.*, **33**, 45-49.

Sud, Y.C., J. Shukla, and Y. Mintz, 1988: Influence of land surface roughness on atmospheric circulation and precipitation: a sensitivity study with a general circulation model. *J. Appl. Meteor.*, **27**, 1036-1054.

Webster, P.J., 1983: Large scale structure of the tropical atmosphere. In *Large Scale Dynamical Processes in the Atmosphere.* B.J. Hoskins and R.P. Pearce, Eds. Academic Press, New York.

Williams, M., 1990: Forests. Chapter 11 in: *The Earth as Transformed by Human Action: Global and Regional Changes in the Biosphere over the Past 300 Years*, B.L. Turner et al. Eds, 179-202.

Zhang, T., 1994: Sensitivity properties of a biosphere model based on BATS and a statistical-dynamical climate model. *J. Climate*, **7**, 890-913.